



Lacustrine coquinas and hybrid deposits from rift phase: Pre-Salt, lower Cretaceous, Campos Basin, Brazil



Vinicius Carbone Bernardes de Oliveira^{a,b,*}, Carlos Manuel de Assis Silva^a,
Leonardo Fonseca Borghi^b, Ismar de Souza Carvalho^b

^a Petrobras Research and Development Center (CENPES), Avenida Horacio de Macedo, 950, Ilha do Fundao – Cidade Universitaria, Rio de Janeiro, RJ, 21949-915, Brazil

^b Universidade Federal do Rio de Janeiro, Centro de Ciências Matemáticas e da Natureza, Instituto de Geociências, Departamento de Geologia, Programa de Pós-graduação em Geologia, Av. Athos da Silveira Ramos, 274, Bloco F, Ilha do Fundao – Cidade Universitaria, Rio de Janeiro, RJ, 21949-900, Brazil

ARTICLE INFO

Keywords:

Pre-salt
Rift sedimentation
Coquinas
Hybrid deposits
Lower cretaceous

ABSTRACT

This study presents a facies characterization, facies succession and conceptual depositional model of the Coqueiros Formation, Lower Cretaceous of Campos Basin, based on core analyses of two wells. WELL-1 is a shallow water drilling located at south of Campos Basin within the Badejo structural high, and WELL-2 is an ultra deep water drilling located at north, over the “External High”. Ten carbonate facies, three siliciclastic facies, two magnesium clay mineral rich facies and two hybrid facies were identified. The carbonate facies were defined as rudstone, grainstone, packstone and mud supported carbonate rock, composed of bivalves, ostracods, and rare gastropods. Bivalve shells, mostly disarticulated with distinct degrees of fragmentation, characterized the main components of the ten carbonate facies. The siliciclastic facies are sandstones and mudstones, which occur locally. The magnesium clay rich facies is composed by stevensitic claystone and arenites. The mixture of bioclasts, siliciclastic grains, stevensite ooids and peloids constitute hybrid facies. The depositional processes involved waves and storm currents, as well as storm refluxes and tectonically-driven gravitational deposits, which mixed particles from different basinal sites producing the hybrid facies. The conceptual depositional model for each geological setting were elaborated based on facies stacking pattern analysis. A hybrid ramp in rift setting, studied in WELL-1, is characterized by carbonate, argillaceous, siliciclastic and hybrid successions, suggesting a strong terrigenous influence and variation of the lake water chemistry. An isolated bioclastic high in a rift setting, studied in WELL-2, is basically constructed by bioclastic sequences with local occurrence of siliciclastic mudstones deposited from hypopycnal plumes in relatively deep water. The extraordinary dominance of bivalve mollusks occurred during the lower Aptian stage in Campos Basin, in an active rift basin, with robust bioclastic productivity within protected basement highs. In structures near to the lake border, predominated siliciclastic and hybrid rock sequences as a result of high structural gradients and terrigenous input. Isolated highs from lakeshores were protected from external terrigenous influence. In lacustrine deep water bioclastic and hybrid arenites were deposited as fans generated by gravitational flows triggered by destabilization of shallower water deposits during episodic storms and tectonic activities. This study of the coquina deposits constructional model within a nearshore and also in a offshore lacustrine system is a useful knowledge for the understanding of coquina reservoir distribution and is applicable in the exploratory investigation of new areas with correlate lacustrine systems.

1. Introduction

The recent discoveries of giant petroleum accumulations within coquinas of the Pre-Salt in Santos and Campos basins (Mello, 2008;

Petersohn and Abelha, 2013; Carlotto et al. 2017), endorsed a new geological characterization of these reservoirs. At the moment, coquinas have been well investigated inside oil fields located in shallow waters of Campos Basin (Bertani and Carozzi, 1985a; Dias et al. 1988;

* Corresponding author. Petrobras Research and Development Center (CENPES), Avenida Horacio de Macedo, 950, Ilha do Fundao – Cidade Universitaria, Rio de Janeiro, RJ, 21949-915, Brazil.

E-mail addresses: viniciuscarbone@petrobras.com.br, carbone.bernardes@gmail.com (V.C.B.d. Oliveira).

<https://doi.org/10.1016/j.jsames.2019.102254>

Received 3 April 2019; Received in revised form 28 June 2019; Accepted 28 June 2019

Available online 04 July 2019

0895-9811/ © 2019 Published by Elsevier Ltd.

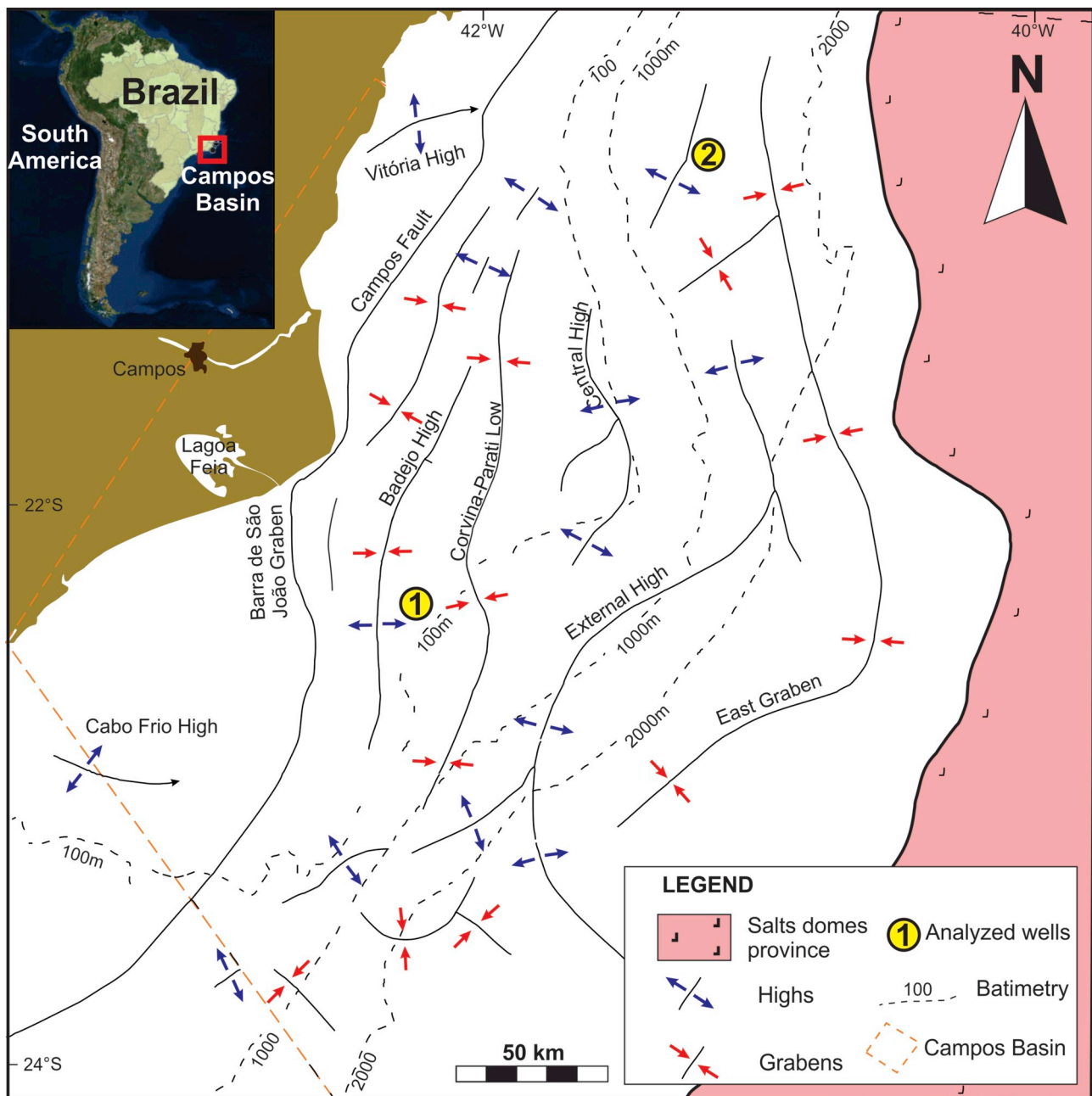


Fig. 1. Studied wells and their locations in a structural map of the Campos Basin, Brazil (modified from Rangel and Martins, 1998).

Carvalho et al. 2000; Bruhn et al. 2003).

In the geological record, beyond the coquinas of Santos and Campos basins coquinas from Eocretaceous are known in the Sergipe-Alagoas Basin (Figueiredo, 1981; Azambuja et al., 1998; Kinoshita, 2007; Tavares et al., 2015) and in the Toca Formation, in the Congo Basin, Africa (Dale et al., 1992; Harris, 2000). At present, no ideal analogue has been found for the understanding of how coquinas form Campos

Basin were formed. However, modern analogues are known and, despite several peculiarities, can be used to understanding shell deposition processes, such as bivalves accumulations in Shark Bay, in Australia (Jahnert et al. 2012) and gastropods deposits in Lake Tanganyika (Cohen, 1989b; Tiercelin et al., 1994; Soreghan and Cohen, 1996).

The current study comprehend the result of a comparative sedimentological study from cores of two wells in Campos Basin. WELL-1 is

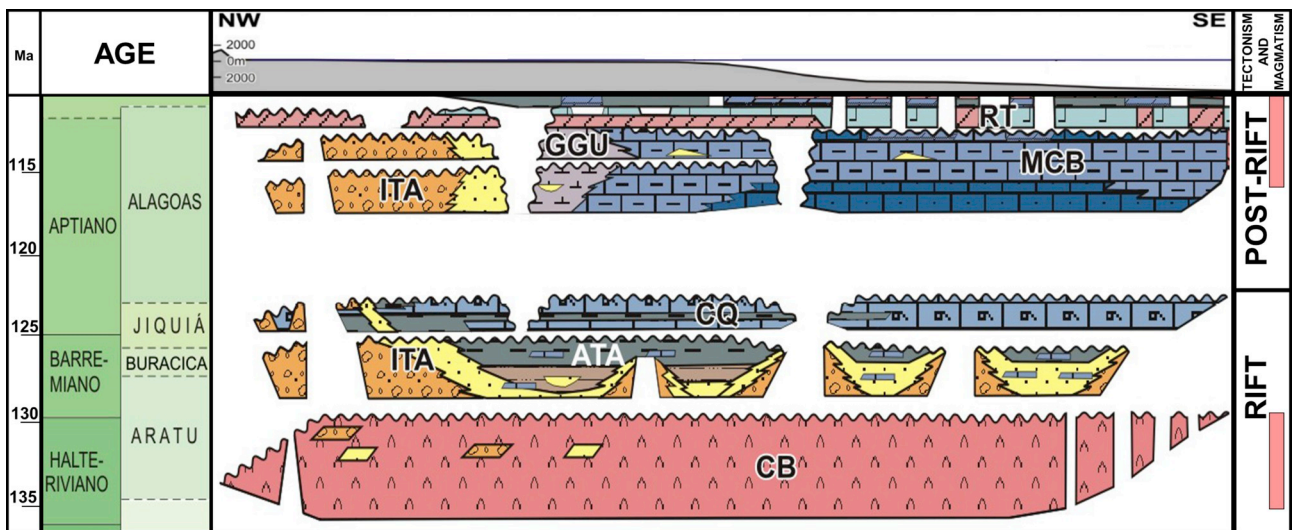


Fig. 2. Stratigraphic chart of the Campos Basin, focusing on the presalt interval (modified from Winter et al. 2007). The evaporitic sequence from the Retiro Formation (RT), overlapping the carbonates of the Macabu Formation (MCB). The Coquina Sequence, Coqueiros Formation (CQ), was deposited in the rift phase during the Jiquia local stage (Aptian-Barremian). Underneath the Coqueiros Formation, sandstone and mudstones of the Atafona Formation (ATA) and basalts of the Cabiunas Formation (CB). In the proximal portion, conglomerates and sandstones of the Itabapoana Formation (ITA).

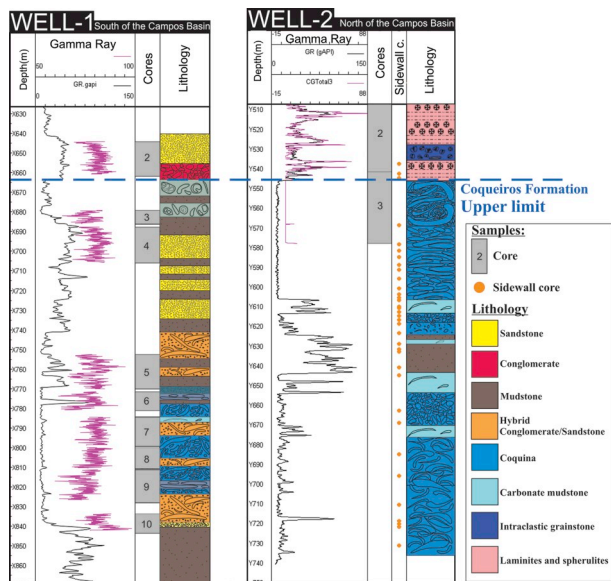


Fig. 3. Studied data: 8 cores from WELL-1 (105.9 m), 1 core (31.5 m) and 27 sidewall cores from WELL-2 and 183 described thin sections.

located on the Badejo High, in shallow water, in the south of Campos Basin, in Linguado Field. WELL-2 is situated over the “External High”, in ultra-deep waters (depth greater than 1000 m) in the north of Campos Basin, in Parque das Baleias area (Fig. 1). The aim of this work is to describe and characterize the sedimentological facies, and analyze

the facies succession in order to propose the depositional model in two distinct paleogeographic emplacement where lacustrine mollusk shells were deposited with distinct terrigenous influence during the rift phase of Campos Basin.

The results envisages a better understanding of the sedimentary processes inside contrasting depositional systems of the two settings supporting interpretation of facies occurrence in areas such as Buzios and Mero fields, in the Pre-Salt of Santos Basin.

2. Geological setting

The Campos Basin, located on the Southeast Brazilian continental margin, originated during the Early Cretaceous, as a result of the Gondwana Supercontinent break-up which occurred after a super-extensional volcanic activity that comprehend the extrusive basalts which cover large areas from the Parana Basin in Brazil and Karoon Basin in Africa (Conceição et al. 1988; Segev, 2002; Dias, 2005).

During the rift phase, the tectonic pattern was characterized by horsts, grabens and half-grabens, originated by synthetic and antithetic normal faults activity oriented preferentially NE-SW (Dias et al., 1990). Structural highs are the focal point for hydrocarbon migration and accumulation in the Pre-Salt sequence. Badejo high is located in proximal shallow water with northward dip (Chang et al. 1992). Badejo oil accumulation was discovered in 1975 (Tigre et al., 1993; Bruhn et al, 2002). The “External High” is a ultra-deep water positive feature that cross the basin from the north to the south. The exploratory campaign on the External High looking for Pre-Salt oil accumulations started in 2003 when the technology of ultra-deep water drilling rigs was available (Gomes et al. 2002; Carminatti et al. 2008; Dehler et al. 2016).

The Campos Basin sedimentar content can be divided into three supersequences: rift, post-rift and drift, which were deposited above the basalt lava flows of the Cabiunas Formation (Winter et al. 2007). In

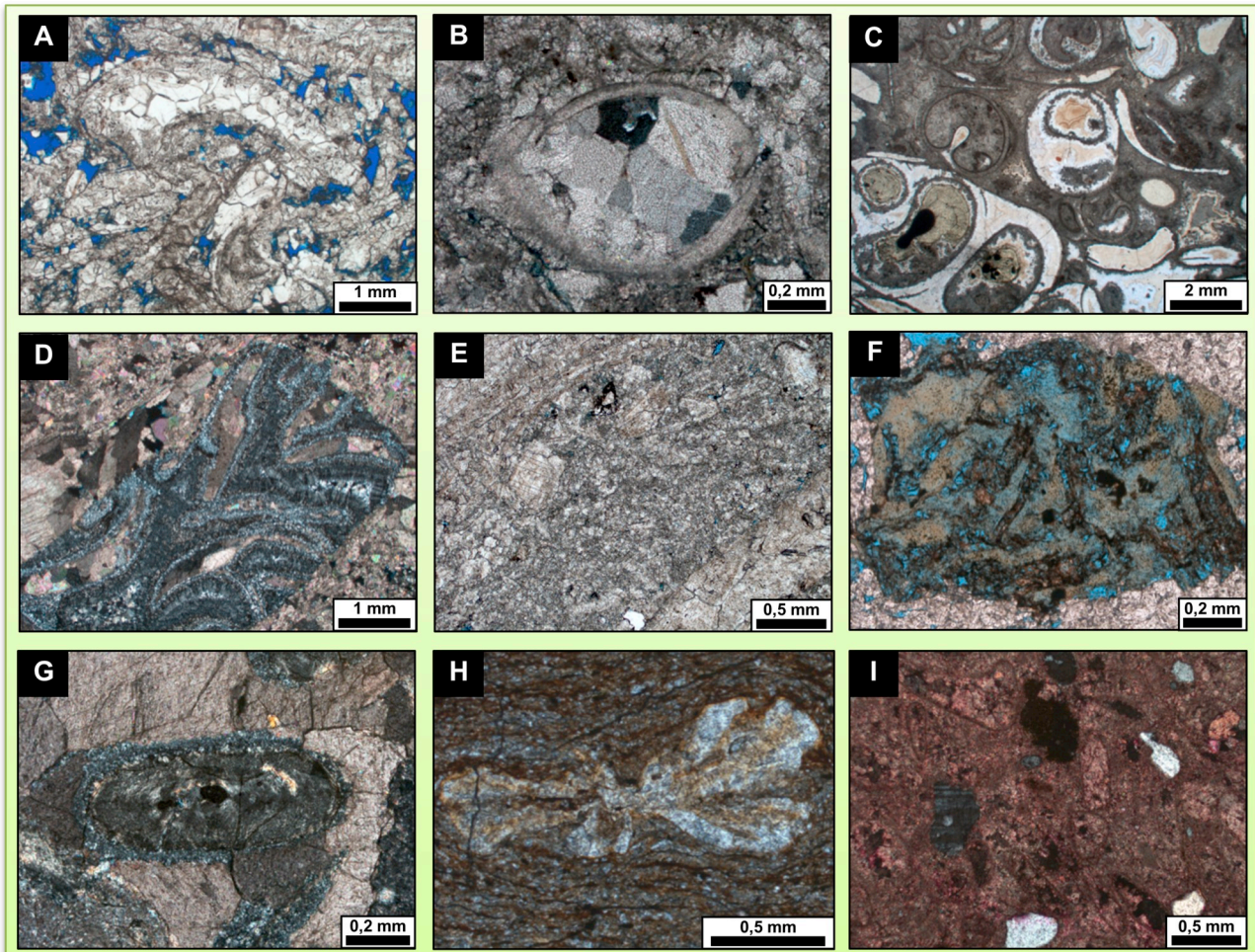


Fig. 4. Photomicrographs of the main components of Coqueiros Formation rocks in the studied wells. A) bivalve shells (WELL-1); B) ostracodes (WELL-1); C) gastropods (WELL-1); D) silicified coquina intraclast (WELL-2); E) recrystallized micrite (WELL-2), F) igneous rock fragment (WELL-2), G) stevensite ooids (WELL-1), H) a fossil vertebrae (WELL-1), I) siliciclastic grains < 0,5 mm (WELL-1).

Campos Basin, Pre-Salt reservoirs are represented by the rift coquinas from the Coqueiros Formation and by the sag lacustrine carbonates from the Macabu Formation. Above the carbonate sequences the Retiro Formation composed of evaporites is the main seal for the oil accumulations (Fig. 2).

The Coqueiros Formation was deposited during the late Barremian-early Aptian (Jiquia local stage, Winter et al. 2007). This formation is characterized by shale layers intercalated with coquinas deposits. The term coquina was defined by Schaffer (1972) as accumulations of shells and/or shell fragments deposited by the action of some transport agent. Shells concentration can also be formed by winnowing (Kidwell, 1986; Fick et al. 2018). The coquinas are bioclastic rudstones, grainstones and packstones, composed dominantly of bivalves varying from 0.3 to 5.0 cm in length, with low faunal diversity. Gastropods, ostracodes, pollen, spores, bone fragments, fish teeth and scales, as well as

fragments of stromatolites and laminites of microbial origin are also constituents of these deposits (Bertani and Carozzi, 1985a; Abrahão and Warme, 1990; Carvalho et al., 1995).

3. Material and methods

This work analyzed data from two wells in the Campos Basin. WELL-1 is located 80 km of the coast of the Rio de Janeiro State, in a water depth of 100 m, on the Badejo Structural High in the south of the basin. WELL-2 is located 75 km off the coast of the Espírito Santo State, in a water depth of 1300 m, over the External High structure, in the North of the Campos Basin (Fig. 1). WELL-1 recovered eight cores, totalling 105.9 m total of rock, and WELL-2 recovered one 31.5 m core length, and 27 sidewall cores.

This sedimentological study was undertaken using 1:20 macroscopic

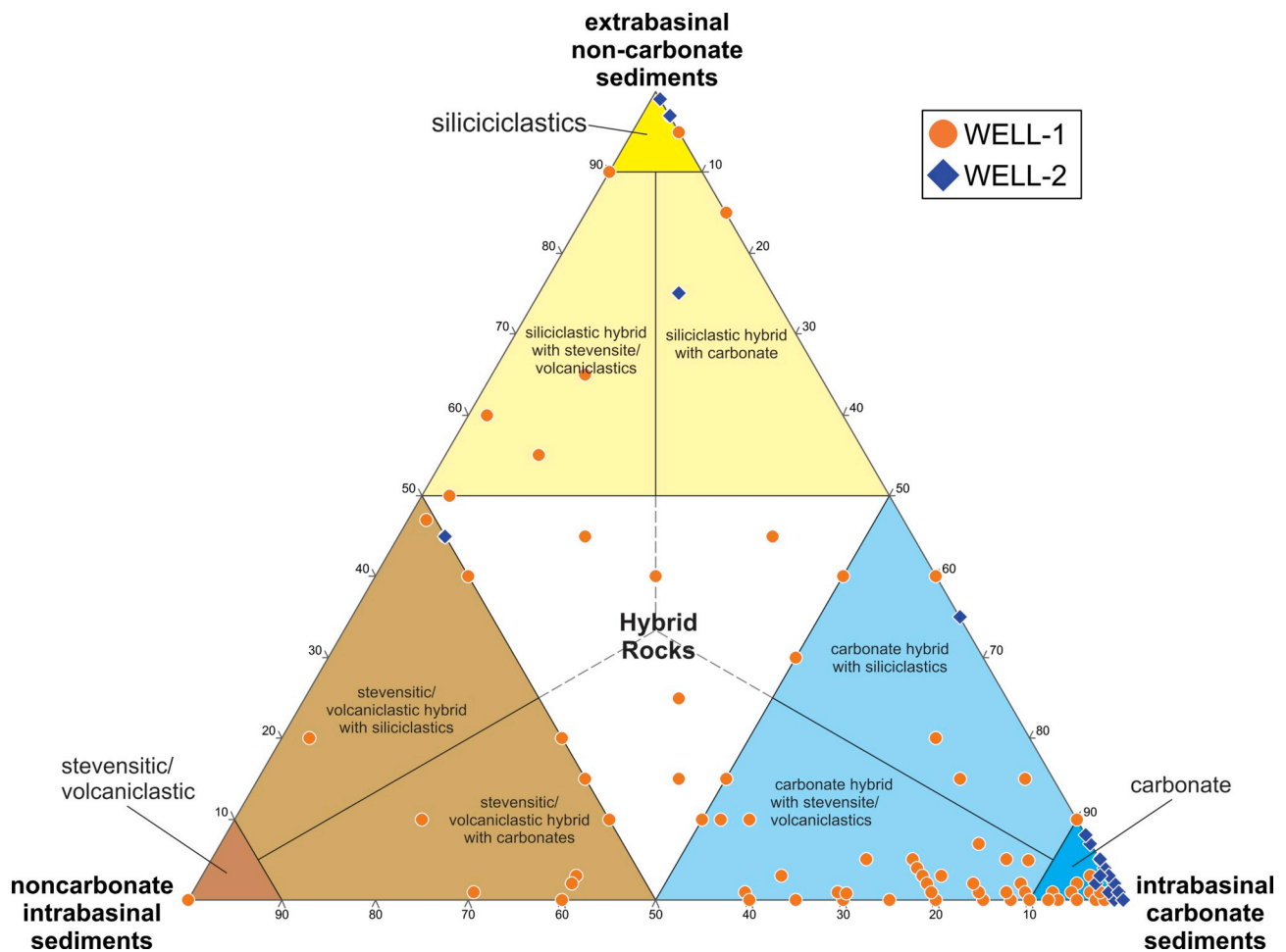


Fig. 5. Ternary diagram proposed to classify the studied rocks, based on constituent's composition. Wells one and two are represented by 179 points inserted on the diagram. The diagram represents non-carbonate extrabasinal, non-carbonate intrabasinal and carbonate intrabasinal (see text for more explanation).

scale core analysis taking into account the sedimentary structures, textures and stacking pattern. The petrographic analysis was performed using an optical microscopy, and visual quantitative analysis applied to describe and study of 180 thin sections (Fig. 3). The facies classification was based on the rock composition, particles size and sorting, and taphonomy, when shells were present. Carbonate rocks were classified using Dunham (1962) and Embry and Klovan (1971) schemes. The taphonomic features considered are shell articulation, degree of fragmentation, rounding, packing, sorting, orientation and mud presence. Then, the facies was named according to the concepts of Selley (1970).

X-ray diffraction analyses (XRD), were performed at the Petrobras Research Center on 39 samples using the analytical protocols of analysis and interpretation described in Brown and Brindley (1980).

4. Results

4.1. Facies analysis

The studied rocks in both wells are composed mainly by intrabasinal carbonates (bivalves, intraclasts, ostracods, gastropods and ooids) followed by clay peloids and ooids, siliciclastic grains, vertebrate fossils and volcanic rock fragments (Fig. 4).

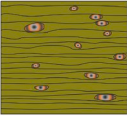


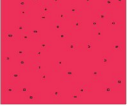
Peloids and ooids are composed of authigenic clay minerals such as smectite, kerolite, kerolite-smectite and also presented micro-layers of illite-stevensite, illite, kaolinite and sepiolite. These grains composed of clay minerals occurred as alternated laminas or micro-layers remarkable in WELL-1. WELL-2 presented a notable content of clastic input occurring as silt-sized grains.

Table 1
Facies descriptions and environment interpretations from the studied wells sedimentary sequence.

Facies Box	Facies	Name	Occurrence	Description	Interpretation
CARBONATE FACIES					
	Rm	massive, poorly sorted, bivalve rudstone	WELL-1 and WELL-2	Rocks supported by shells and shell fragments, with modal size between pebbles and very coarse sand, poorly-sorted, disarticulated, with variable fragmentation, without preferential orientation	Deposit formed by storm-induced currents and waves (Carvalho et al., 2000; Jahnert et al., 2012), and tectonically-driven gravitational flows (Goldberg et al., 2017).
	Ro	organized bivalve rudstone	WELL-1 and WELL-2	Rudstones formed by moderated fragmented bivalves with a preferred orientation, with shells and shell fragments, moderately selected. Sparse, micritic and coquina intraclasts.	High energy environments, above fairweather wave base, with waves and currents (Nagle, 1967; Kidwell et al., 1986; Kidwell and Bosence, 1991; Muniz, 2013).
	Rf	broken and rounded shells rudstone	WELL-1 and WELL-2	Rudstones with broken and rounded bivalve shells, shells disarticulated and fragmented, granules to very coarse sand, well sorted. The rock can be stratified or massive.	High energy environment, above fairweather wave base, on the swash zone (Muniz, 2013).
	Rg	bivalve-gastropod rudstone	WELL-1	Rudstones composed by gastropods and disarticulated bivalves with whole or low fragmented shells, poorly sorted, massive. Subordinately, quartz and feldspar, silt and very fine grained sand.	Gastropods, when compared to bivalves, would live in environments with higher salinity and alkalinity, and less availability of calcium (Harris, 2000). Lag deposits in littoral platform are constituted by gastropod and bivalve mixed (Tiercelin et al., 1994).
	Rw	bivalve rudstone with whole shells	WELL-1	Rudstone composed by articulated or disarticulated low fragmented bivalves shells. Rocks are massive, poorly sorted.	Small remobilization of the bivalves living places, with absence of carbonate mud related to winnowing processes (Folk, 1962; Muniz, 2013).
	Ru	bivalve rudstone with micritic matrix	WELL-2	Rudstone with with matrix of carbonate mud, composed by disarticulated or articulated shells, whole or broken, poorly selected	Deposits in moderate to low energy environments, in protected or relatively deep areas, below fairweather wave base (Muniz, 2013).
	Gf	broken and rounded shells grainstone	WELL-1 and WELL-2	Grainstone consist of bivalve, ostracods and intraclasts, high fragmented and rounded, with modal size very coarse sand, moderate to well sorted.	Very broken and reworked shells are related to shallow environments, with continuous traction by action of waves and currents (Folk, 1962; Muniz, 2013).
	P	ostracod-bivalve packstone	WELL-2	Packstone are massive, medium to coarse grained, moderately sorted, composed by ostracodes, bivalves, and in minor proportion, feldspar grains and volcanic rocks fragments.	The ostracods rich sediments are deposited in low lake periods, in saline alkaline environment, where the mud matrix was remobilized by weak currents or wind generated waves (Bertani and Carozzi, 1985a).
	Mc	mud-supported carbonate rock	WELL-1 and WELL-2	This facies is composed by mudstones, wackestones and floatstone with mud matrix. This rocks present bivalve and ostracod, articulated or disarticulated, whole or low fragmented, supported by carbonate mud,	This facies is interpreted as formed in low energy environments, which may be related to protected or relatively deeper areas, below the fairweather wave base (Flügel, 2004; Muniz, 2013).
	U	chert, crystalline limestone and dolostone	WELL-1 and WELL-2	This facies is identified by rock with unrecognizable precursor rock, such as chert, crystalline limestone, dolostone	Dolomitization and silicification are processes that can take place in low energy lakes and shallow lakes that may be exposed (Bustillo et al., 2002; Bustillo et al., 2017). These process can occur during eodiagenesis (Bertani and Carozzi, 1985b; Bustillo, 2010).
HYBRID FACIES					
	Ah	hybrid arenite	WELL-1	Rock with modal size smaller than 2 mm, formed by a mixture of bioclastic, siliclastic, and stevensite grains, without a single particle type with more than 90% of the total composition.	The mixture of bioclasts with siliclastic grains may occur due to continental contribution (Tavares et al., 2015). Sediment from differentes origins can be mixed by gravitational re-deposition (Goldberg et al., 2017) and storm-induced currents (Carvalho et al., 2000).
	Ch	hybrid conglomerate	WELL-1	Rock with modal size greater than 2 mm, formed by a mixture of bioclastic, siliclastic, and stevensite grains, without a single particle type with more than 90% of the total composition.	
MAGNESIUM CLAY FACIES					
	As	stevensitic arenite	WELL-1	Rocks with more than 90% of stevensitic ooids and peloids, medium to coarse sand grained, moderately sorted, massive.	Precipitation in highly alkaline conditions in lacustrine or palustre environment, with some agitation by waves or currents (Rehim et al., 1986; Pozo and Casas, 1999; Herlinger et al., 2017).

(continued on next page)

Table 1 (continued)

Facies Box	Facies	Name	Occurrence	Description	Interpretation
	Cs	stevensitic claystone	WELL-1	Claystone, with incipient lamination, composed by dolomitized stevensitic clay lamellae, with quartz, feldspar and mica angular grains, silt to very fine sand frained, and rare articulated ostracods.	Precipitation in highly alkaline conditions in lacustrine or palustre environment (Rehim et al., 1986; Pozo and Casas, 1999; Herlinger et al., 2017).
SILICICLASTIC FACIES					
	S	sandstone	WELL-1	Fine to medium sandstones, moderately to well selected, massive, occasionally with fining upward and ripples, constituted by quartz, feldspar, mica, opaque grains, igneous rock fragment, subangular to subrounded, with high sphericity.	Flood-induced hyperpycnal flows that trigger turbidity currents (Zhang and Scholz, 2015).
	Mg	gray mudstone	WELL-1 and WELL-2	Gray mudstone, some may be slightly greenish, constituted by quartz, feldspar and mica grains, angular, silt and very fine sand, in a clay matrix. Total organic carbon higher than 3 wt%.	Fine siliciclastic grains come from the continent due to hypopycnal plumes, related to floodings in high water levels (Bates, 1953; Mulder and Alexander, 2001) and are deposited by decantation in lake bottom (Carvalho et al., 2000)
	Mr	red mudstone	WELL-1	Red mudstone, constituted by quartz, feldspar and mica grains, angular, silt and very fine sand, in a clay matrix. Total organic carbon higher than 0,03 wt%.	Low-energy settings, in marginal or deep lacustrine area, with prolonged exposure and oxidizing (Bertani, 1984; Abrahão and Warme, 1990).

The primary composition of rocks of WELL-1 and WELL-2 are plotted on a ternary diagram quantified by visual estimation of the rock constituents (Fig. 5). This diagram was elaborated basing on the categories first proposed by Zuffa (1980), and the ones more recently proposed by Armententi et al. (2016) and Goldberg et al. (2017). The vertices of the diagram represent the compositional end members non-carbonate particles of extrabasinal origin, carbonate particles of intrabasinal origin and non-carbonate particles of intrabasinal origin. The non-carbonate extrabasinal particles are represented by quartz and feldspar grains and fragments of volcanic rocks, while carbonate intrabasinal particles are composed by bivalves and ostracod bioclasts, coquina intraclasts, gastropods and phosphatic fragments. Non-carbonate intrabasinal particles include clay peloids and ooids as well as volcanic rock fragments.

Rocks with more than 90% of a single component are defined as siliciclastic sandstones and mudstones, stevensite/volcanic enriched arenites and carbonate rocks. Rocks mixed with more than one component were designated as hybrid, which were named according to the main composition followed by reference to the secondary principal component. Inside the central triangle are plotted the hybrid rocks as proposed by Zuffa (1980).

Rocks described in the WELL-1 (Fig. 5), were predominantly hybrid due to the presence of non-carbonate extrabasinal particles (usually quartz and feldspar grains) and non-carbonate intrabasinal particles (clay ooids and peloids), besides the occurrence of carbonate rocks, composed of bioclasts, and siliciclastic rocks, like sandstones and siliciclastic mudstones. In WELL-2 carbonate rocks predominate with more than 90% of bioclastic intraclasts, mostly bivalve shells. Igneous rock fragments occur in minor proportions. The rare siliciclastic rocks of this well are mudstones.

Considering the two wells, seventeen facies were identified: ten carbonate facies, three siliciclastic facies, two argillaceous facies and two hybrid facies (Table 1 and Fig. 6). The main objective for facies identification based in a descriptive criteria assured a concise sedimentological reconnaissance searching for the recognition of the elements of a proximal and distal lacustrine depositional system.

Facies definition were based in the lithological composition, but in the case of clastic argillaceous and hybrid rocks the grain size was also applied in order to distinguish the facies. In the case of carbonatic rocks with original texture recognizable a subdivision was made using an extension for the principal lithology followed by the mud or particle supported content. To differentiate bivalve supported rock, taphonomic features were applied, such as shell articulation, degree of fragmentation, rounding, packing, sorting, orientation and mud presence.

4.1.1. Massive, poorly sorted, bivalve rudstone

This lithofacies is characterized by particle supported framework, composed of bivalve shells and shell fragments larger than 2 mm, with modal size between pebble and very coarse sand, poorly-sorted, disarticulated, with variable degree of fragmentation (mainly moderated to highly fragmented), with chaotic fabric (Fig. 7). Locally, few ostracods were identified. Especially in WELL-2 was visible the preservation of primary porosity (space inter-shells particles) and in a minor degree vugs generated by the shell dissolution.

These rudstones were found in WELL-1 and WELL-2, as layers with 20 cm to 1 m thick presenting abrupt or erosional bases, homogeneous structureless shells arrangement with or without fining upward particle size. The layers can form amalgamated packages of 20 cm to 1 m thick or can occur intercalated with other facies.

These deposits may be interpreted as being re-deposited by

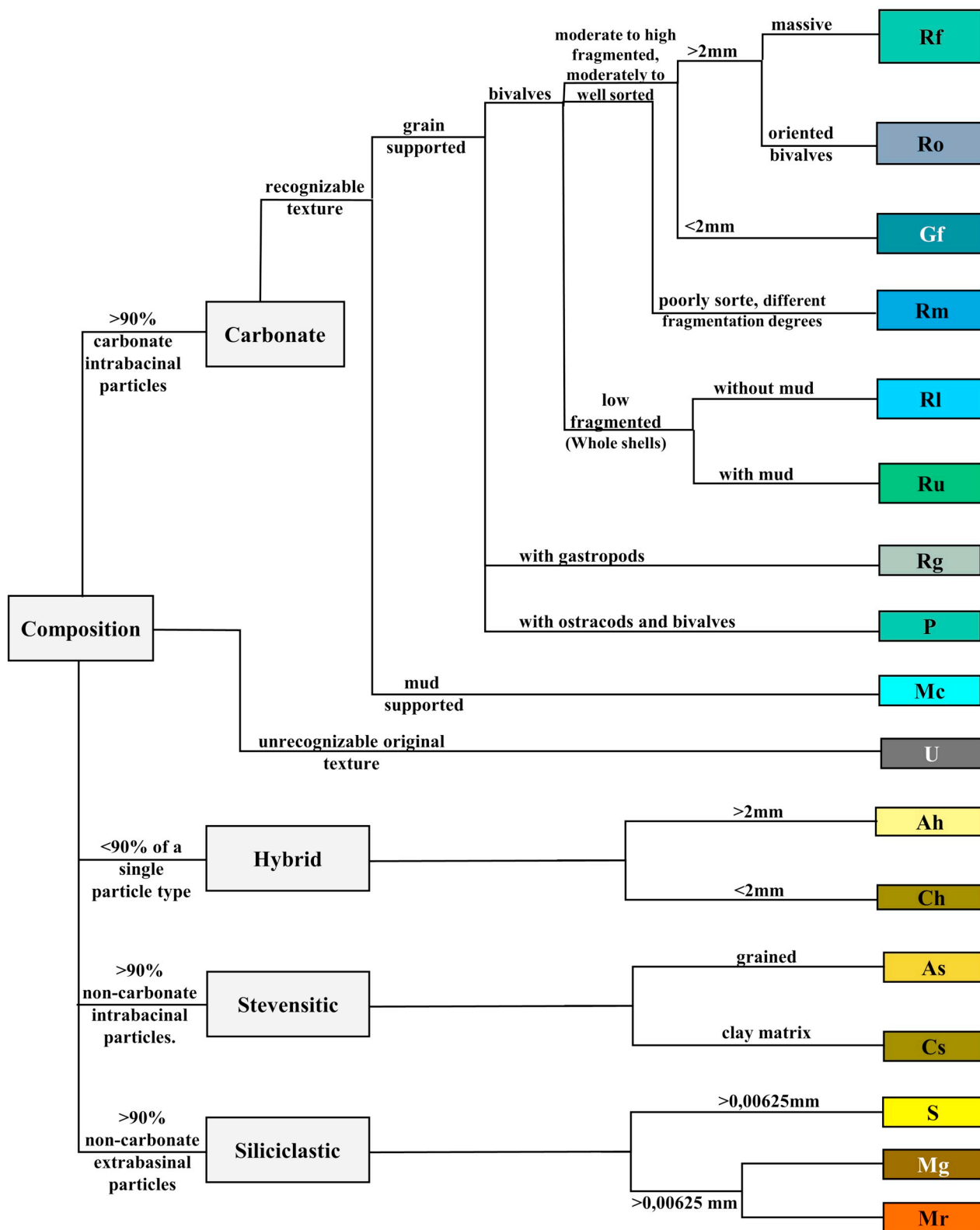


Fig. 6. Facies classification systematics for analyzed rocks, based on composition, granulometry, texture and taphonomy. For facies abbreviations, see Table 1.

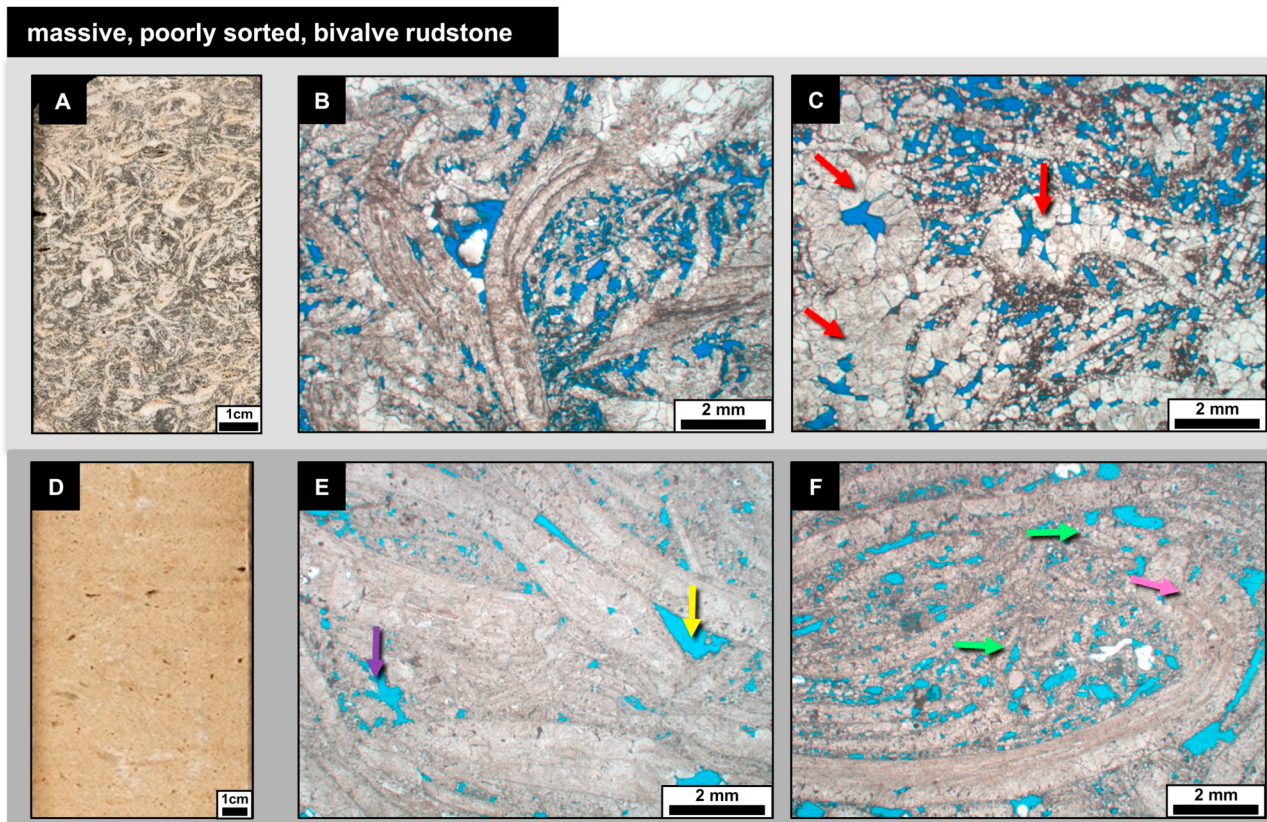


Fig. 7. Massive, poorly sorted, bivalve rudstone. A) Macroscopic aspect of the facies, WELL-1. B) Textural aspect, seen in a photomicrograph, WELL-1. (uncrossed polarizers). C) Bivalve dissolved and partially cemented by blocky calcite (red arrow) (uncrossed polarizers). D) Macroscopic aspect of the facies, WELL-2. E) Poorly sorted bivalve rudstone with interparticle (yellow arrow) and vuggy porosity (purple arrow) (WELL-2, uncrossed polarizers). F) Mixture of whole valves with preserved growth lines and fragmented medium to fine sized bivalves (green yellow) (WELL-2, uncrossed polarizers). (For interpretation of the references to colour in this figure legend, the reader is referred to the Web version of this article.)

gravitational flows because of the mixture of shells with different degrees of reworking such as non-fragmented and articulated shells and rounded broken shells (cf. Goldberg et al. 2017). Massive rudstones with variable degree of fragmentation may be also explained as being formed by storm-induced currents and waves as suggested by Carvalho et al. (2000) and Mizuno et al. (2018). Storms can also have acted as winnowing agents, removing muds and mixing distinct shells population (Cohen, 1989b). In any case, it has been interpreted as generated by episodic high-energy events, like storm waves or gravitational flows.

4.1.2. Organized bivalve rudstone

This facies is characterized by rudstones with moderately fragmented shells with a preferential convex-up orientation (Fig. 8). It presents shells and shell fragments up to 1 cm size, moderately sorted (size usually varies from coarse sand to pebble). The bioclasts are normally densely packed, with some stylolites, and cemented by calcite. Secondly, there are micritic and coquina intraclasts. Locally, cross-statification was recognized in cores. Sparsely, primary porosity can be

preserved and the bioclasts be dissolved.

This lithofacies occurs in both wells studied, as layers up to 50 cm thick, amalgamated or intercalated with massive, poorly sorted, bivalve rudstone.

The organization of shells is interpreted as a response to high-energy environments, with waves and currents (Nagle, 1967; Kidwell et al. 1986; Kidwell and Bosence, 1991). Organized shells can be present in convex-up beach ridges (Jahnert et al. 2012). This facies is interpreted as being deposited by tractive processes due to the action of currents and fair-weather waves.

4.1.3. Broken and rounded shell rudstone

This facies is characterized by rudstones with broken and rounded bivalve shells. The shells are disarticulated and fragmented with up to 4 mm size, with modal size of granule to very coarse sand, moderately to well sorted (size usually varies from coarse sand to pebble), disposed as stratified or massive packages (Fig. 9). This facies is remarked by the higher degree of roundness and sorting. This rudstone is generally

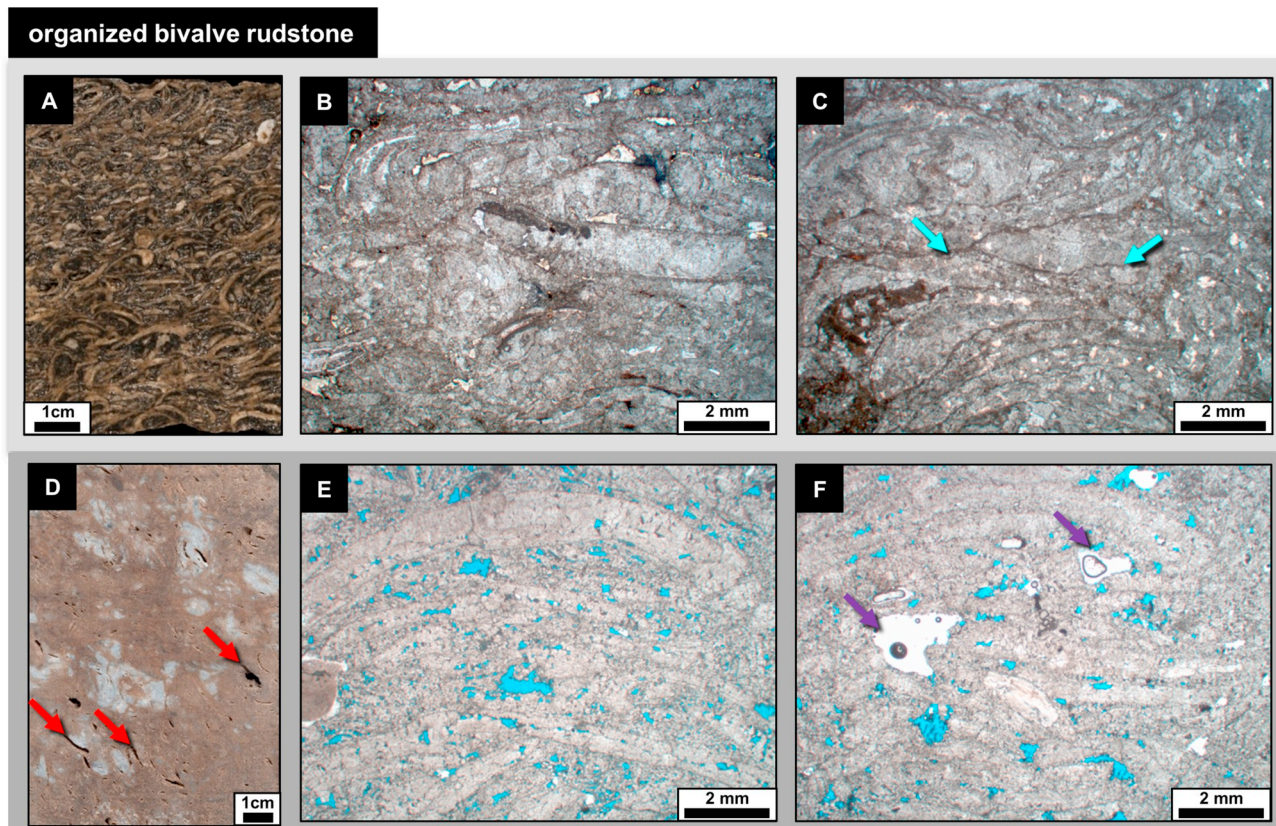


Fig. 8. Organized bivalve rudstone facies. A) Macroscopic aspect of the facies characterized by oriented shells, with prevailing upward convexity (WELL-1). B) Dense packaging bivalve rudstone with oriented shells (WELL-1, uncrossed polarizers). C) Dense packaging oriented bivalve rudstone with stylolites (blue arrows) (uncrossed polarizers). D) Macroscopic aspect of sample, WELL-2, with red arrow indicating moldic and vuggy porosities. E) Oriented bivalve shells (WELL-2, uncrossed polarizers). F) Vuggy porosity (purple arrows) (WELL-2, uncrossed polarizers). (For interpretation of the references to colour in this figure legend, the reader is referred to the Web version of this article.)

highly cemented by calcite with bioclasts and calcite cement sparsely dissolved.

This lithofacies was recognized mainly in WELL-2, occurring as layers up to 20 cm thick, which may be intercalated with organized bivalve rudstone and massive, poorly sorted, bivalve rudstone.

In WELL-2, this rudstone is composed of rounded coquina intraclast, some silicified, and rounded volcanic rock fragments, with minor proportion of ostracods and bivalve shells with micritic borders.

The silicified intraclasts are interpreted as a product from the erosion of previously deposited but uncemented shell beds, but which had been already buried and diagenetically altered. The volcanic rock fragments may be related to intrabasinal volcanism (Bertani and Carozzi, 1985b) or exposure of basement highs, common in rift setting (Muniz, 2013; Goldberg et al. 2017). The broken and rounded shells facies may have been the result of a high-energy environment, above fair-weather wave base, on the swash zone (Muniz, 2013).

4.1.4. Bivalve-gastropod rudstone

This facies is distinguished from the other bivalves rudstones by the presence of gastropods in their composition (Fig. 10). The rudstones are massive, composed of gastropods and disarticulated bivalves with intact or only partly fragmented shells, up to 7 mm in size, and are poorly sorted. Subordinate amounts of silt to fine sand-sized grains also occur. Gastropods are recrystallized by spar calcite, or replaced by quartz and chalcedony. There is intense cementation by calcite in interparticle space.

These rudstones were restricted to the top of WELL-1, in layers of 30–40 cm, which are intercalated with abrupt contacts with mudstone and hybrid arenites. The Coqueiros Formation gastropods belong to the family *Limneidae* (Carvalho et al. 2000). In the Congo Basin in Africa, the presence is due to periods of higher salinity and alkalinity (Harris, 2000).

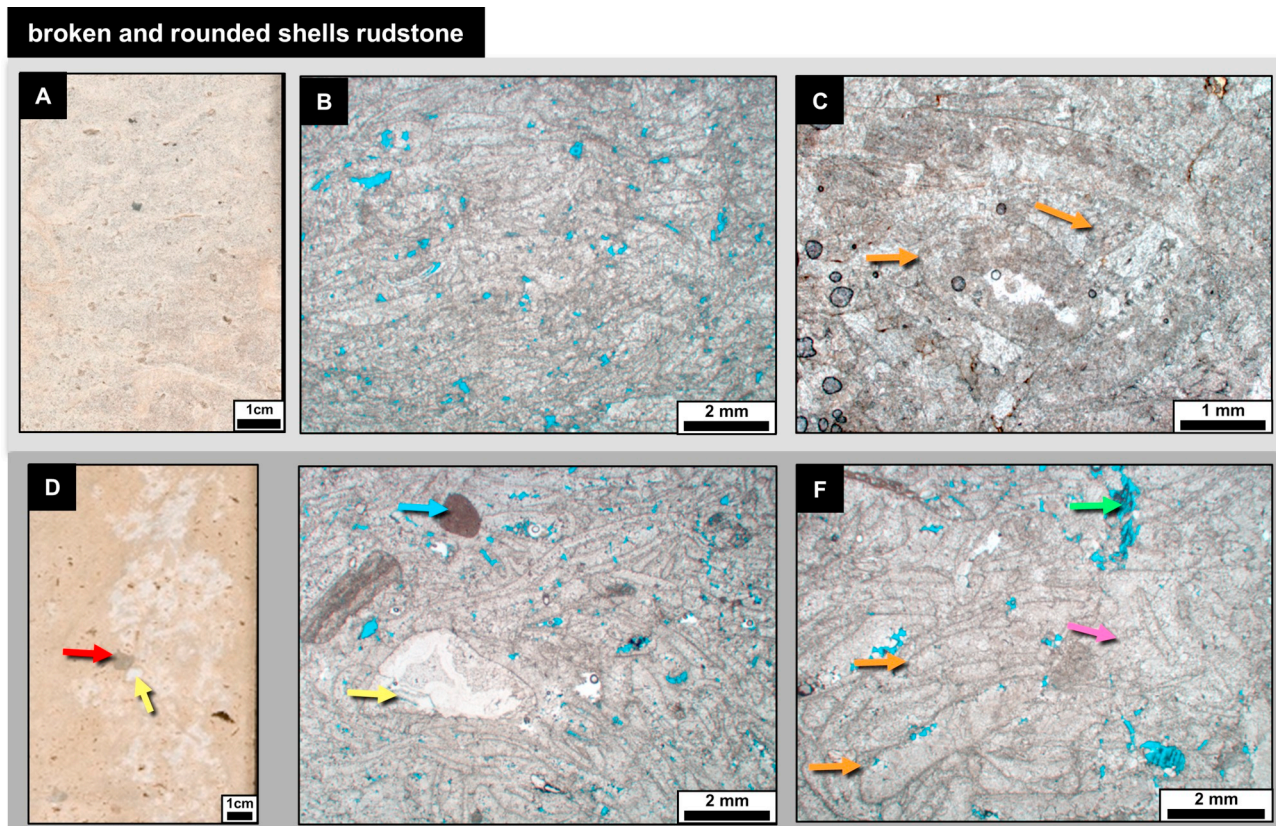


Fig. 9. Broken and rounded shells rudstone. A) Macroscopic aspect, WELL-1. B) Densely packed bivalve rudstone, WELL-1 (uncrossed polarizers). C) Rounded shells (orange arrows) (uncrossed polarizers). D) Macroscopic core aspect, WELL-2, with rounded shells, intraclast (red arrow) and chert fragment (yellow arrow). E) Broken and rounded shell rudstone with micritic intraclast (blue arrow) and chert fragment (yellow arrow) (WELL-2, uncrossed polarizers). F) Rounded shells (orange arrows), with calcite cement (pink arrow) and vuggy pore by dissolution (green arrow) (WELL-2, uncrossed polarizers). (For interpretation of the references to colour in this figure legend, the reader is referred to the Web version of this article.)

4.1.5. Bivalve rudstone with low degree of fragmentation

This facies is identified by rudstone composed dominantly of disarticulated bivalves or with low degree of fragmentation (Fig. 11). Subordinately, disarticulated bivalves up to 1 cm, are mixed with non-fragmented ostracods. In general, these rocks are massive and poorly sorted, with modal size from granule to pebble and are intensely cemented by calcite. Macroscopically, it is commonly presents mottled aspect. Shells generally are recrystallized, but some growth lines were preserved.

The occurrence of disarticulated bivalve shells with a low degree of fragmentation suggests a short transport of the bivalves from their living places. Non-fragmented coquinas occur related to winnowing and dynamic bypassing domains (Fick et al. 2018). The winnowing process, which produces bioclasts size sorting when shells and fragments fall in a dynamic water body, may be responsible for absence of carbonate mud (Folk, 1962; Muniz, 2013).

4.1.6. Bivalve rudstone with micritic matrix

This facies is characterized by a rudstone composed of bivalves, with carbonate mud rich matrix (Fig. 12). It is composed primarily of poorly sorted (medium sand-pebble sized) disarticulated shells. However, some articulated, whole shells (some broken) do occur, some of which can reach more than 1 cm length. Bedding is structureless (massive). Normally, the micrite was partially replaced by dolomite or neomorphised to spatic calcite.

These rudstones was characterized only in WELL-2, preferentially in the base of the well, associated with mud-supported carbonate rock, occurring as mudstone and wackestone, and bivalve rudstone with a low degree of fragmentation.

Coquinas with low fragmentation and micritic matrix were interpreted as deposited in deep lacustrine environment in the Morro do Chaves Formation, in the Sergipe-Alagoas Basin, Brazil (Tavares et al. 2015). Bivalve rudstone with micritic matrix was interpreted here as

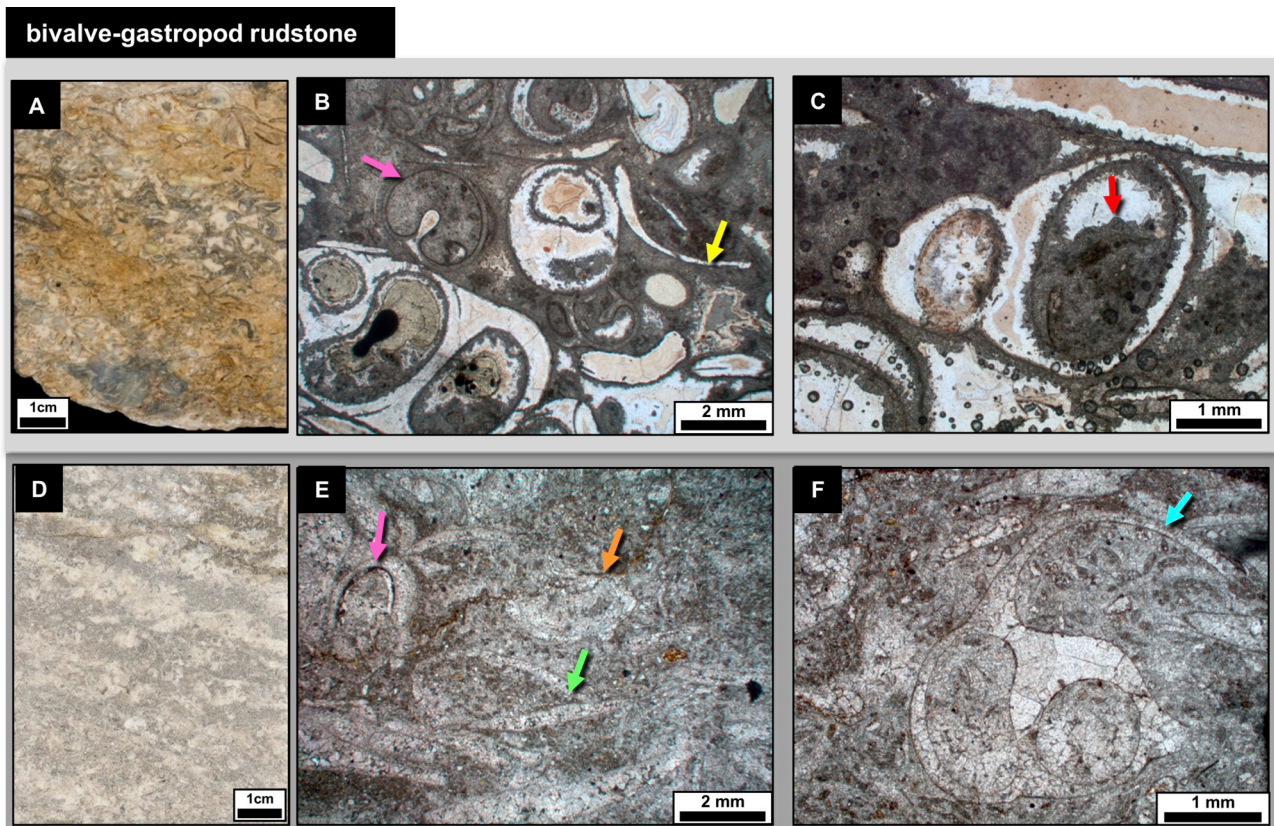


Fig. 10. Bivalve-gastropod rudstone. A) Macroscopic aspect of the facies, WELL-1. B) Photomicrographs from WELL-1, with gastropods (pink arrow) and articulated bivalve (yellow arrow) (uncrossed polarizers). C – Silicified gastropod with a geopetal infilling (WELL-1, uncrossed polarizers). F) Macroscopic aspect, WELL-1. E) Gastropod (pink arrow), articulated bivalve (green arrow), with stylolites (orange yellow). F) Non-fragmented gastropod (WELL-1, uncrossed polarizers). (For interpretation of the references to colour in this figure legend, the reader is referred to the Web version of this article.)

been deposited in moderate to low energy environments, probably in protected areas or relatively deeper, below fair-weather wave base (Muniz, 2013).

4.1.7. Broken and rounded shells grainstone

This facies is characterized by bivalve grainstones in which the bivalves are highly fragmented and rounded (Fig. 13). These grainstones consist of bivalve fragments, ostracods and carbonate intraclasts, with a very coarse sand, which are moderately to well sorted (size ranging from coarse sand to pebble). The grainstones can be laminated or massive. Commonly, the shells have micritic coating and are cemented by blocky calcite.

This lithofacies were described in both wells, as layers up to 70 cm thick, intercalated mainly with broken and rounded shells rudstone and organized bivalve rudstone. In WELL-2, micritic and coquina intraclasts, some silicified, and volcanic rock fragments are common.

These grainstones differ from the broken and rounded shells rudstones because they are supported by shell fragments smaller than 2 mm,

possibly because they were subjected to water high-energy conditions for a long time. Very broken and reworked shells are related to shallow environments, with continuous abrasion of shells by action of waves and transport by longshore currents (Folk, 1962; Muniz, 2013).

4.1.8. Ostracod-bivalve packstone

This packstone is composed of ostracods, bivalves and, in minor proportion, feldspar grains and volcanic rocks fragments and micritic matrix (Fig. 14). In general, the rock is massive and moderately sorted, with grain size ranging from medium to coarse sand. The bioclasts are very fragmented, sub-rounded to rounded, and may have micritic coatings. Bioclasts are intensely recrystallized with highly cemented by interparticle calcite.

This facies only occurs in WELL-1 locally in 20 cm thick layers, with abrupt base, or with transitional contact with mud-supported carbonate rocks.

Bioclastic packstones may be formed by turbidity currents, storms, or as washover fans in lagoons (Muniz, 2013). The ostracod rich

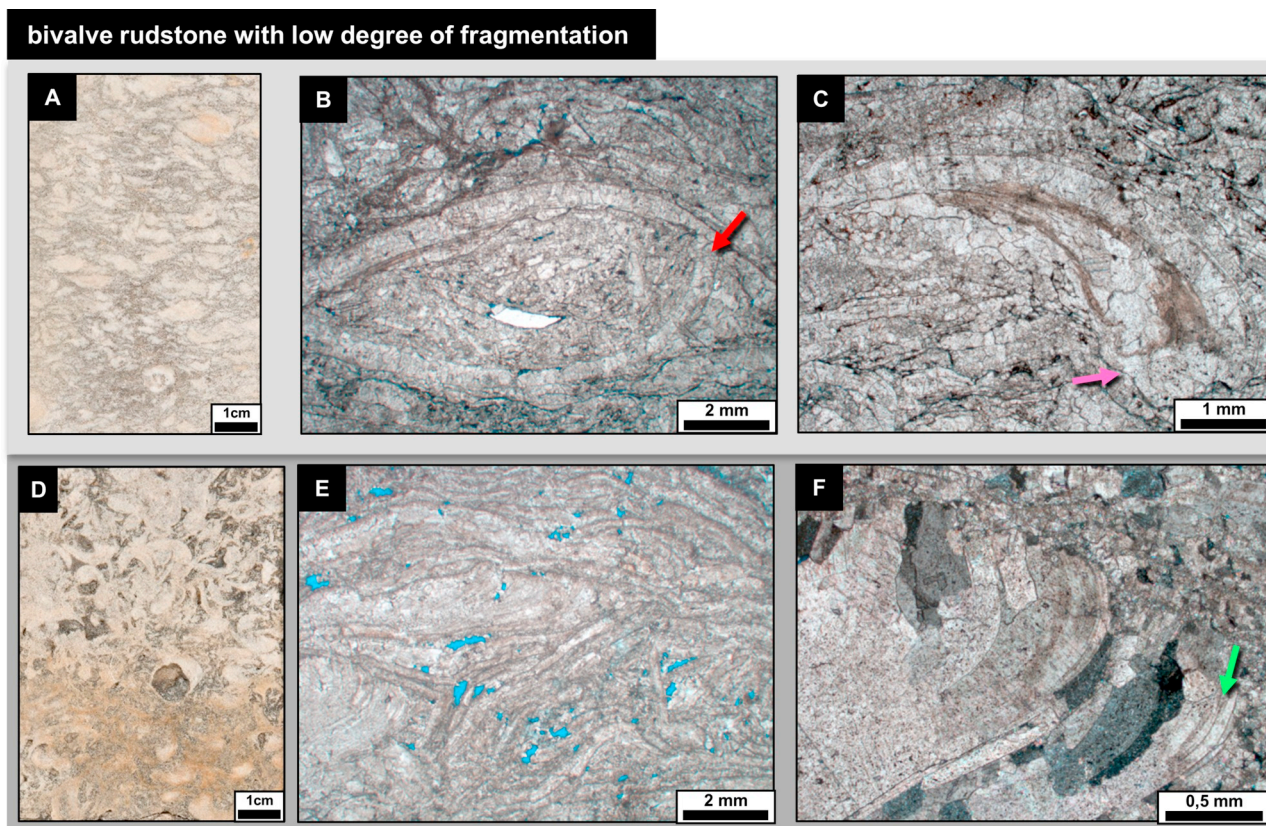


Fig. 11. Bivalve rudstone with low degree of fragmentation. A) Macroscopic aspect of the facies, WELL-1. B) Articulated bivalve shell from WELL-1 (red arrow) (uncrossed polarizers). C) Non-fragmented disarticulated bivalve shell (pink arrow) (uncrossed polarizers). D) Core detailed photo from WELL-1, with an articulated bivalve (red arrow). E) Bivalve rudstone with low degree of fragmentation from WELL-2 (uncrossed polarizers). F) Disarticulated bivalve shell recrystallized with some growth lines preserved (uncrossed polarizers). (For interpretation of the references to colour in this figure legend, the reader is referred to the Web version of this article.)

sediments were deposited in periods after the maximum water level, when water conditions started to change transforming, in saline alkaline environment (Bertani and Carozzi, 1985a). The mud matrix was remobilized by weak currents or wind generated waves (Bertani and Carozzi, 1985a).

4.1.9. Mud-supported carbonate rock

The facies included mudstones, wackestones and floatstones with disperse bivalves and ostracods, articulated or disarticulated, whole or fragmented, supported by carbonate mud matrix, which normally is intensely recrystallized to fine calcite or replaced by dolomite (Fig. 15). Rare silt grains of quartz, feldspar and mica were associated with opaque minerals, mostly pyrite. Most of the rocks are massive, but some may exhibit incipient lamination.

These rocks occur locally in both wells, being more often in sidewall cores of the sampled basal portion of WELL-2, where it occurs inter-layered with mudstones and bivalve rudstone with micritic matrix.

Rocks supported by the carbonate mud matrix with little amount of siliciclastic grains were formed in a low energy offshore environment (Bertani and Carozzi, 1985a). Inorganic dolomitization of carbonate mud may be related to shallow lakes (Bustillo et al. 2017). This facies is interpreted having been in low energy environments, which may be related to protected or relatively deeper areas, below the fair-weather wave base (Flügel, 2004; Muniz, 2013).

4.1.10. Chert, crystalline limestone and dolostone

These rocks are formed by intense replacement/recrystallization of the primary constituents leaving no recognizable original texture and structure (Fig. 16).

Cherts are composed of chalcedony, microcrystalline quartz and/or coarsely crystalline quartz. The crystalline limestones, in general, present a fine to medium-crystalline mosaic of calcite, sometimes medium to coarse blocky calcite. Dolostone are constituted by fine to medium rhombohedral, subhedral to euhedral dolomite.

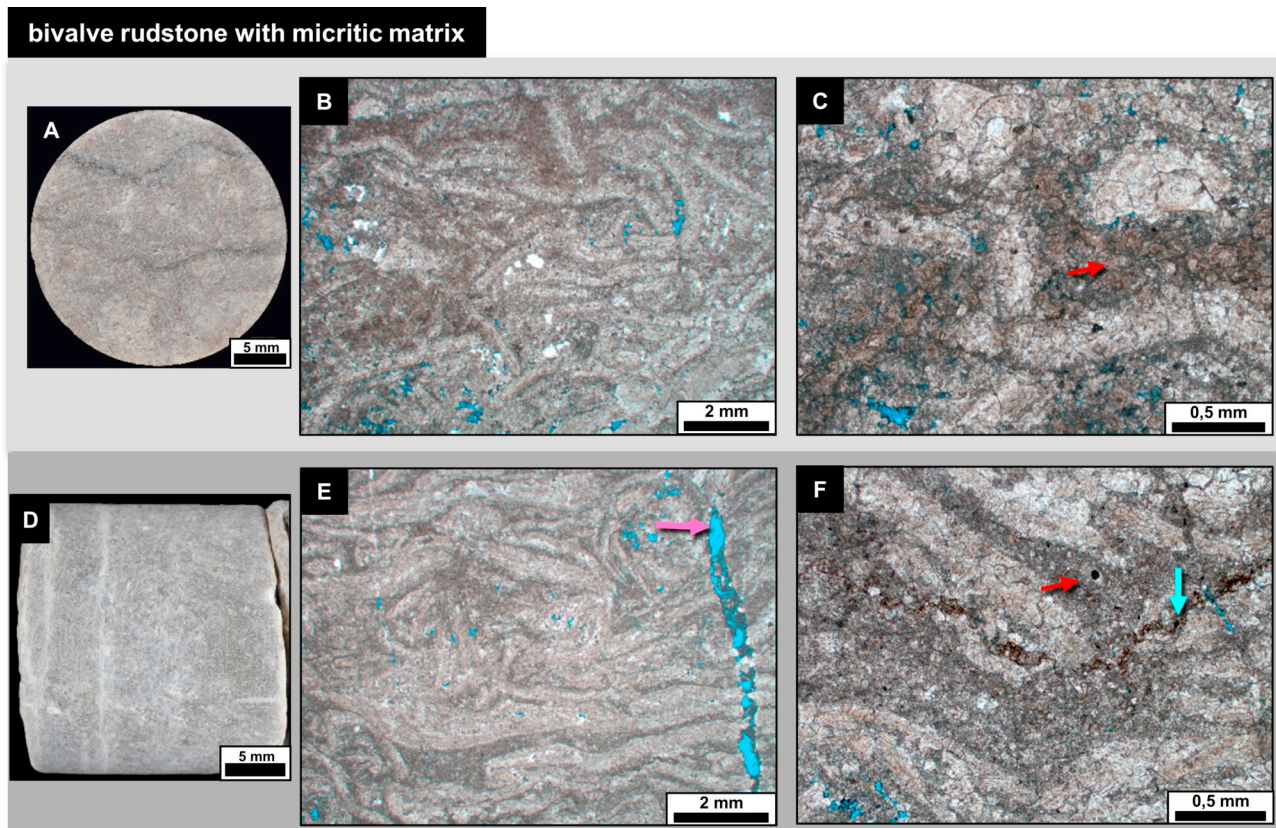


Fig. 12. Bivalve rudstone with micritic matrix. A) Macroscopic aspect of a sidewall core, WELL-2. B) Photomicrograph from WELL-2 (uncrossed polarizers). C) Micrite replaced by dolomite (red arrow) (uncrossed polarizers). D) Macroscopic aspect of a sidewall core, WELL-2. E) Photomicrograph from WELL-2, whit a dissolution channel (pink arrow) (uncrossed polarizers). F) Micrite replaced by dolomite (red arrow) and stylolites (blue arrow) (WELL-2, uncrossed polarizers). (For interpretation of the references to colour in this figure legend, the reader is referred to the Web version of this article.)

In some cases, carbonate remnants of the original constituents are identified, such as disarticulated ostracods. In addition to intense processes of calcite recrystallization and dolomite or silica replacement, dissolution can occur, which generated vugs. Some of these rocks are brecciated.

These facies are observed in both wells, but more commonly in WELL 2. These rocks have a high degree of recrystallization of the bioclasts and micrite to other calcite habits. Calcite replacement by dolomite and quartz is common, as well as cementation by calcite, dolomite and quartz. These diagenetic processes were intense enough to change completely the depositional texture and structure.

Dolomitization and silicification are processes that can take place in low energy lakes and shallow lakes that may be exposed (Bustillo et al., 2002; Bustillo et al., 2017). These processes can be generated during eodiagenesis (Bertani and Carozzi, 1985b; Bustillo, 2010).

4.1.11. Hybrid arenite and conglomerate

Hybrid arenite and conglomerate are characterized by a mixture of grains of different compositions in variable proportions, but not containing more than 90% of a single particle type (Fig. 17 and Fig. 18). The hybrid rocks studied are poorly sorted and may be composed of bivalve and ostracod bioclasts, stevensite ooids and peloids, igneous rock fragments and, in minor proportion, feldspar, quartz and mica grains. In general, rocks are poorly sorted and massive. In the hybrid conglomerates, the granule and pebble size particles are disarticulated bivalves that reach up to 3 cm in length. These rocks are intensely cemented by calcite and dolomite. Some particles are dissolved, generating molds.

This facies occurs only in WELL-1 in successive layers 30–50 cm thick, and can be massive or graded fining upwards, with abrupt or erosive base.

The mixture of bioclasts with siliciclastic grains may be related to terrigenous flows in the lake, as observed in rift lacustrine coquinas of

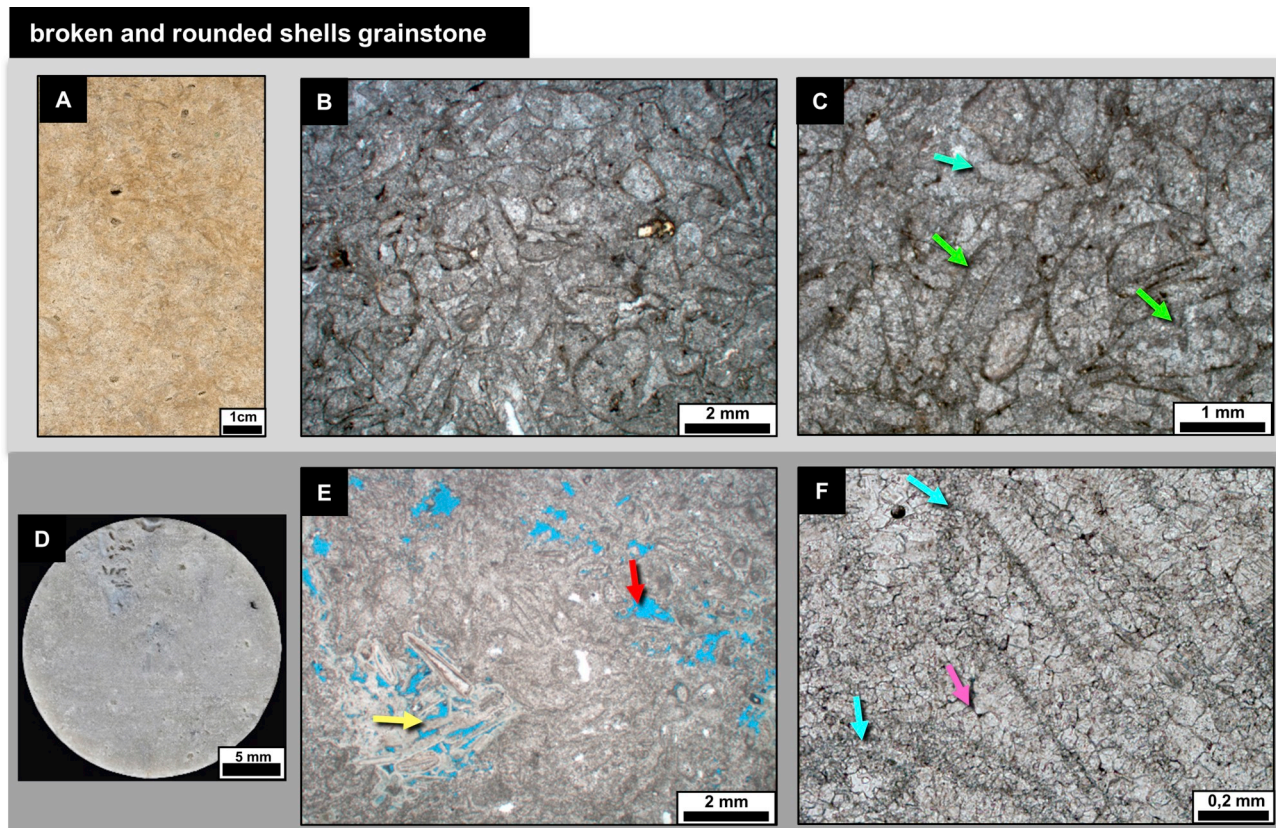


Fig. 13. Broken and rounded shells grainstone. A) Macroscopic aspect of the facies, WELL-1. B) Photomicrograph of a broken and rounded shells grainstone from WELL-1 (uncrossed polarizers). C) Broken and rounded shells (green arrow), cemented by blocky calcite (blue arrow). D) Macroscopic aspect of a sidewall core, WELL-2. E) Broken and rounded shells grainstone from WELL-2, silicified (yellow arrow) and dissolved (red arrow) (uncrossed polarizers). F – Shells with micritic edge and blocky calcite interparticle (uncrossed polarizers). (For interpretation of the references to colour in this figure legend, the reader is referred to the Web version of this article.)

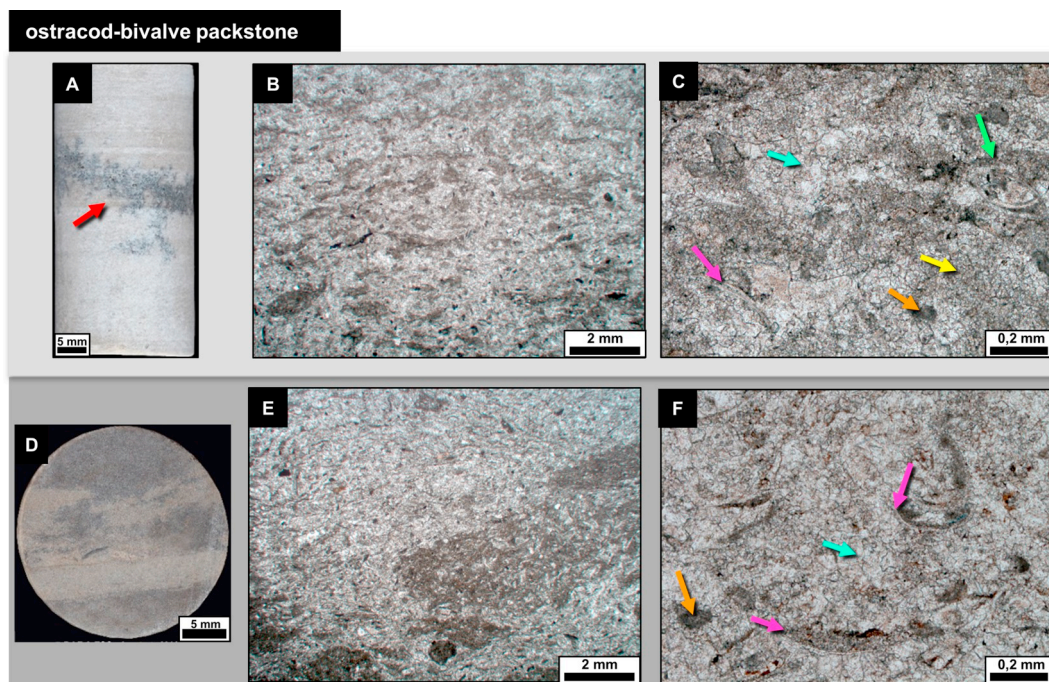


Fig. 14. Ostracod-bivalve packstone. A) Macroscopic aspect of a sidewall core with high dissolution feature (red arrow), WELL-2. B) Photomicrograph from WELL-1 (uncrossed polarizers). C) Detail of an ostracod packstone: disarticulated ostracod (pink arrow), articulated ostracod (green arrow), peloid (orange arrow), calcite cement (blue arrow), micrite recrystallized (yellow arrow) (uncrossed polarizers). D) Macroscopic aspect of a sidewall core, WELL-2. E) Photomicrograph from WELL-2 (uncrossed polarizers). F) Detail of packstone composition: ostracod (pink arrows), peloid (orange arrow), calcite cement (blue arrow) (uncrossed polarizers). (For interpretation of the references to colour in this figure legend, the reader is referred to the Web version of this article.)

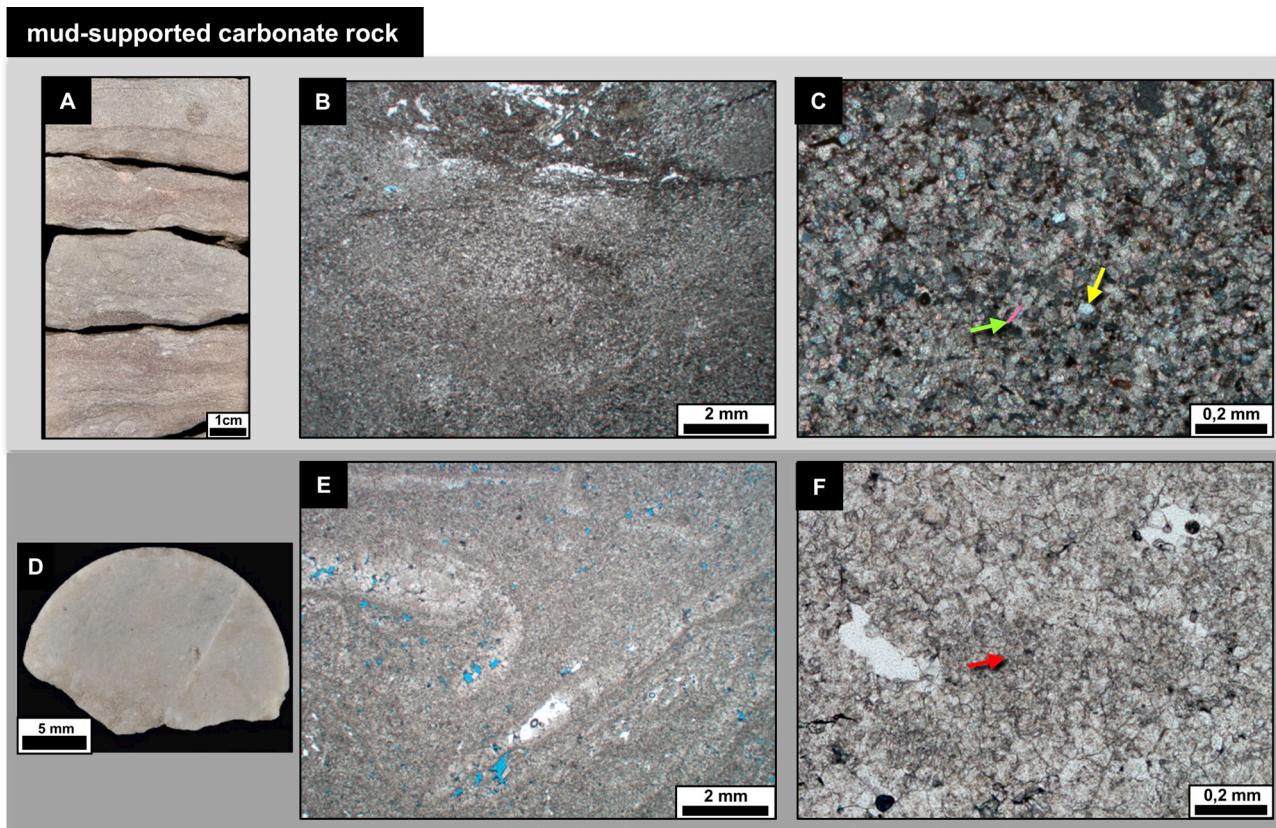


Fig. 15. Carbonate mud supported facies. A) Macroscopic aspect of the facies, WELL-1. B) Photomicrograph from WELL-1 (uncrossed polarizers). C) Carbonate mud recrystallized with some quartz (yellow arrow) and mica grains (green arrow) (WELL-1, crossed polarizers - XP). D) Macroscopic aspect of a sidewall core, WELL-2. E) Bioclastic floatstone with micritic matrix from WELL-2 (uncrossed polarizers). F) Recrystallized micrite (red arrow) (WELL-2, uncrossed polarizers). (For interpretation of the references to colour in this figure legend, the reader is referred to the Web version of this article.)

the Sergipe-Alagoas Basin (Tavares et al. 2015). Siliciclastic sediments can also be mixed with shells due to tectonic episodes that mixed and gravitationally re-deposited sediments in half-grabens troughs (Goldberg et al. 2017), and also by storm-induced currents (Carvalho et al. 2000).

4.1.12. *Stevensitic arenite*

This facies is constituted by rocks with more than 90% of stensitic ooids and peloids. The sediments are medium to coarse grained sand, moderately sorted and with massive structure (Fig. 19). Ooids are characterized by a concentric, isopachous and submillimetric lamination, which in some cases are dissolved or replaced by calcite. The ooid cores can be formed by ostracods, and rarely they are policomposed. In minor proportion, there are disarticulated and articulated ostracods, as well as quartz and feldspar grains. The ooids consist of kerolite, sepiolite, smectite and interlayered kerolite-smectite, according to X-ray diffraction. The rock is intensely cemented by dolomite and calcite.

These arenites are rare, but when it does occur it forms in layers with abrupt and straight contacts and in beds of a maximum thickness of 20 cm, which were displayed intercalated with argillites and hybrid arenites and conglomerates. This facies occurred only in WELL-1. Stevensitic arenite sequences with approximately 50 m thick were also described in other wells in the Campos Basin (Herlinger et al. 2017).

The clay minerals were precipitated in lacustrine or palustrine environment in alkaline conditions which are very different of the ideal conditions for bivalve development (Rehim et al. 1986; Pozo and Casas, 1999; Herlinger et al. 2017). The presence of stensitic in Campos Basin is interpreted as precipitated in magnesium-rich lake waters related to contemporaneous volcanism, as observed in modern African lakes and also inferred in the Green River Formation in Wyoming, USA (Baumann et al. 1975, Abrahão and Warme, 1990). Ooids were probable formed in environments with low energy waves or currents (Herlinger et al. 2017).

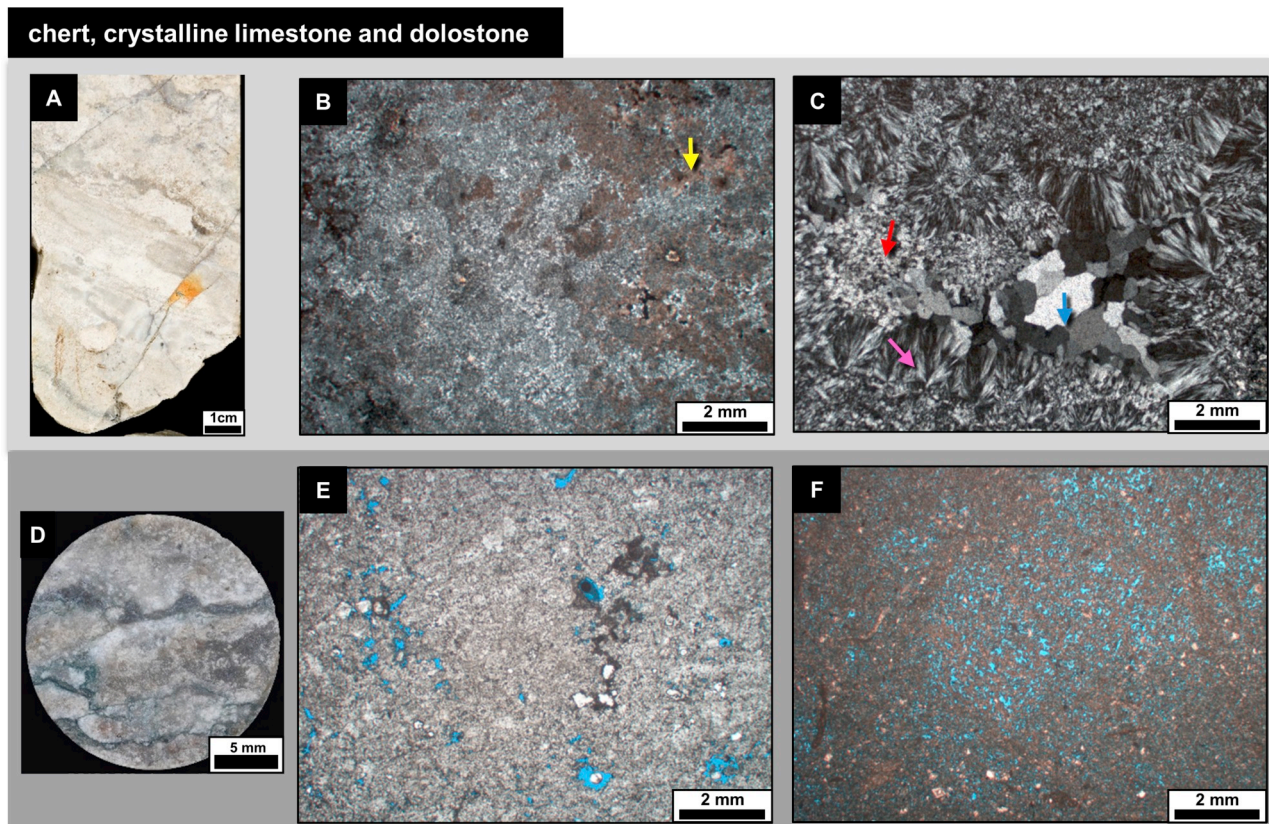


Fig. 16. Examples of chert, crystalline limestone and dolostone. A) Macroscopic aspect of the facies, WELL-1. B) Cherts photomicrographs from WELL-1, with some carbonate remnant (yellow arrow) (XP). C) Chert composition detail: chalcedony (pink arrow), macrocrystalline (blue arrow) and microcrystalline (red arrow) quartz (PX). D) Macroscopic aspect of a sidewall core, WELL-2. E) Crystalline limestone from WELL-2 (uncrossed polarizers). F) Dolostone with high porosity from WELL-2 (uncrossed polarizers). (For interpretation of the references to colour in this figure legend, the reader is referred to the Web version of this article.)

4.1.13. *Stevensitic claystone*

This facies contains incipient lamination and is composed by dolomitized clay rich lamina, quartz, feldspar, mica from silt to very fine sized grains, and rare articulated ostracods, up to 1 mm (Fig. 20). Clay pisolites > 1 cm diameter with carbonate or volcanic rock cores are present. Stevensitic lamellae can rarely occur dissolved. According to X-ray diffraction analyses, the clay minerals present include interlayered illite-stevensite, kaolinite, smectite, kerolite, interlayered kerolite-smectite, sepiolite and illite. Diagenetic pyrite is common.

Stevensitic arenites are rare and were only observed in WELL-1, with small thickness up to 35 cm, intercalated with mudstone, stensivitic arenite, and hybrid conglomerates and arenites.

This claystone was formed in when the lake water were more alkaline, with similar environmental conditions of stensivitic ooids (Bertani and Carozzi, 1985a; Rehim et al. 1986; Pozo and Casas, 1999). Although, stensivitic claystone were generated in lower-energy conditions (Herlinger et al. 2017).

4.1.14. *Sandstone*

This facies is characterized by fine to medium sandstones, some coarse grained, composed of quartz, feldspar, mica, opaque minerals and igneous rock fragment, with subangular to subrounded grains with high sphericity (Fig. 21). Beds are usually moderately to well sorted, massive, occasionally with fining upward grain size and with ripples. The sandstone is commonly intensely cemented by magnesium clay.

These sandstones occurred only found in WELL-1, where it was deposited as layers that can reach up to 1m thick, locally with thinning upward, intercalated with mudstones, and rare, hybrid deposits.

Massive beds, associated with finning and thinning upward sequences are related to alluvial fans (Bertani and Carozzi, 1985a; Dias et al. 1988, Abrahão and Warme, 1990) or flood-induced hyperpycnal flows that trigger turbidity currents (Zhang and Scholz, 2015).

4.1.15. *Gray mudstone*

Gray mudstone sometimes with a greenish tone containing quartz,

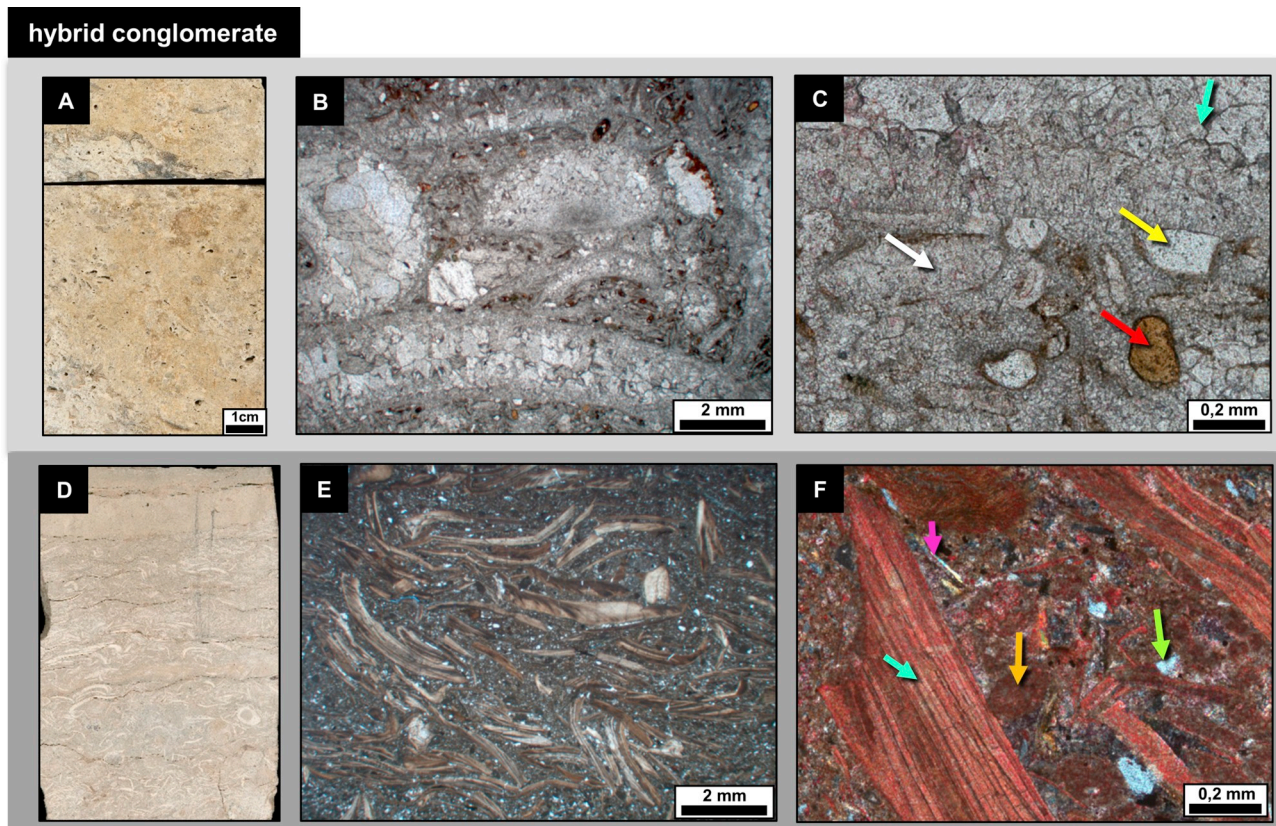


Fig. 17. Hybrid conglomerate facies. A) Macroscopic aspect of the facies, WELL-1. B) Photomicrograph from WELL-1 (uncrossed polarizers). C) Recrystallized bivalve (blue arrow), ostracod (white arrow), quartz grain (yellow arrow) and clay peloid (red arrow). (WELL-1, uncrossed polarizers). D) Macroscopic aspect of the facies, WELL-1. E) Photomicrograph from WELL-2 (uncrossed polarizers). F – Bivalve (blue arrow), peloid (orange arrow), feldspar grain (green arrow) and mica grain (pink arrow) (XP, with alizarin staining). (For interpretation of the references to colour in this figure legend, the reader is referred to the Web version of this article.)

feldspar and mica silt to very fine sized grains, in a clay matrix (Fig. 22). The mudstone can contain ostracod shells, pyrite, and phosphatic fragments, some identified as vertebrate fossils. Commonly, the rocks are laminated, with rare nodules of chalcidony. XRD analysis identified interstratified illite-smectite, chlorite and illite. Total organic carbon content is above 3%.

These mudstones occurred in both wells, although it is more common in WELL-1, where layers occur that can reach 1-m thickness. In WELL-1, this rock commonly appears intercalated with sandstones, while in WELL-2, it occurred intercalated with mud-supported carbonate rock.

Siliciclastic mudstone may be related to distal part of alluvial fans, mud flats in lake margin, or lake center deposits (Bertani and Carozzi, 1985a; Dias et al. 1988, Abrahão and Warme, 1990). These rocks are deposited in low energy conditions with decantation of sediment on the lake bottom (Carvalho et al. 2000). The fine siliciclastic are due to hypopycnal plumes, related to floodings in high water levels (Bates, 1953; Mulder and Alexander, 2001).

4.1.16. Red mudstone

This facies consist of, silt to very fine sand sized quartz, feldspar and mica, with a clay matrix (interstratified illite-smectite, according to XRD analysis). Clay peloids, micritic peloids, and bivalves, ostracods and gastropods non-fragmented shells also occur (Fig. 23). Phosphatic fragments and dispersed autigenic pyrite also occurred. Rocks generally displayed incipient lamination, and, locally, are brecciated. Total organic carbon concentrations are less than 0.03%.

These rocks were only characterized in WELL-1, where it occurred layers of up to 3 m thick, which were interlayered with hybrid rocks, massive bivalve rudstones, organized rudstone and gastropod rudstone.

These mudstones may be associated with low-energy settings, in marginal lacustrine ponds, subjected to prolonged exposure and oxidizing conditions (Bertani, 1984; Abrahão and Warme, 1990).

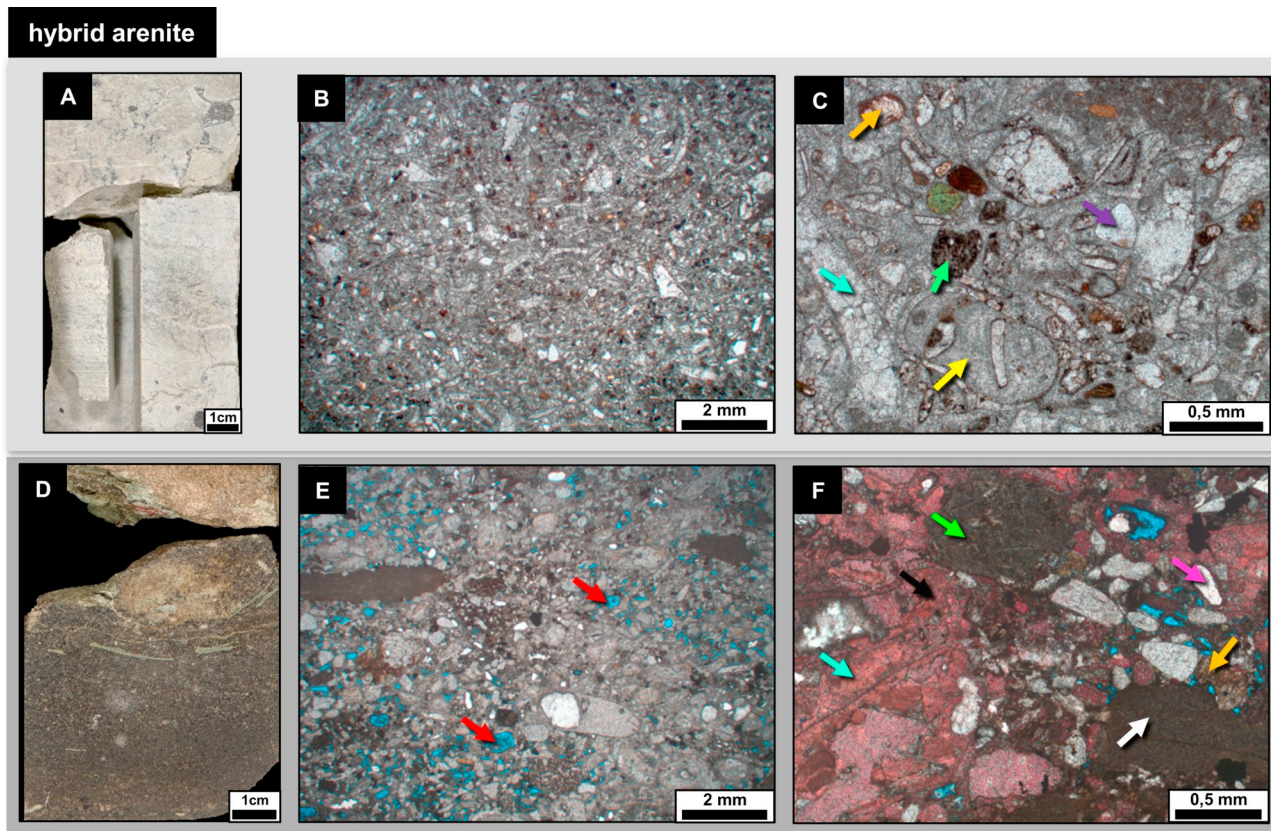


Fig. 18. Hybrid arenite facies. A) Macroscopic aspect of the facies, WELL-1. B) Photomicrograph from WELL-1 (uncrossed polarizers). C) Hybrid arenite composition detail: recrystallized bivalve (blue arrow), feldspar grain (purple arrow), intraclast (yellow arrow), clay peloid (orange arrow), volcanic rock fragment (green arrow) (WELL-1, uncrossed polarizers). D) Macroscopic aspect of the facies, WELL-1. E) Photomicrograph from a hybrid arenite from WELL-2, with some moldic porosity (red arrows) (PP) (uncrossed polarizers). F) Hybrid arenite composition detail: recrystallized bivalve (blue arrow), clay peloid (orange arrow), micritic intraclast (white arrow), quartz grain (pink arrow), volcanic rock fragment (green arrow), and high cementation by calcite (black arrow) (WELL-2, uncrossed polarizers, with alizarin staining). (For interpretation of the references to colour in this figure legend, the reader is referred to the Web version of this article.)

5. Discussion

5.1. Facies succession

In order to interpret depositional models that occurred in the shallow waters in the south of the Campos Basin (WELL-1) and the ultra-deep waters area, in the north of the basin (WELL-2); eight facies successions were proposed based on the facies analysis and stacking patterns. Each facies succession is composed of genetically related facies with environmental significance (Table 2 and Fig. 24).

5.1.1. Carbonate succession 1 – bioclastic bars

Bars succession are characterized by overlapping packages of massive, poorly sorted, bivalve rudstone (Rm), with metric thickness, some with erosive bases and without siliclastic intercalation. Locally, organized bivalve rudstones (Ro) and broken and rounded shells rudstones with coquina intraclasts (Rf) were described. The main porosity

visible were vugs and channels formed by dissolution. This succession was found in both wells. Bioclastic bars composed of massive, poorly sorted, bivalve rudstone occurred in layers as thick as 1 m, forming successions thicker than 10 m, as observed in WELL-2.

Bioclastic bars has been interpreted as formed in high-energy environments from storms (Carvalho et al. 2000; Jahnert et al. 2012; Muniz, 2013). Bioclastic accumulation on highs can also be related to tsunamis produced by tectonic activity during the rift phase (Bryant et al. 1992; Dawson and Stewart, 2007, Freundt et al. 2007, Morton et al., 2007, Massari et al., 2009). Eventually, the bars were exposed and submitted to dissolution. In rift settings, subsidence with continuously generated of accommodation space promoted the stacking of rudstones beds, forming deposits of tens of meters.

5.1.2. Carbonate succession 2 – reworked bioclastic bars

Reworked bioclastic bars are constituted by the intercalation of organized bivalve rudstone with broken and rounded shells rudstone/

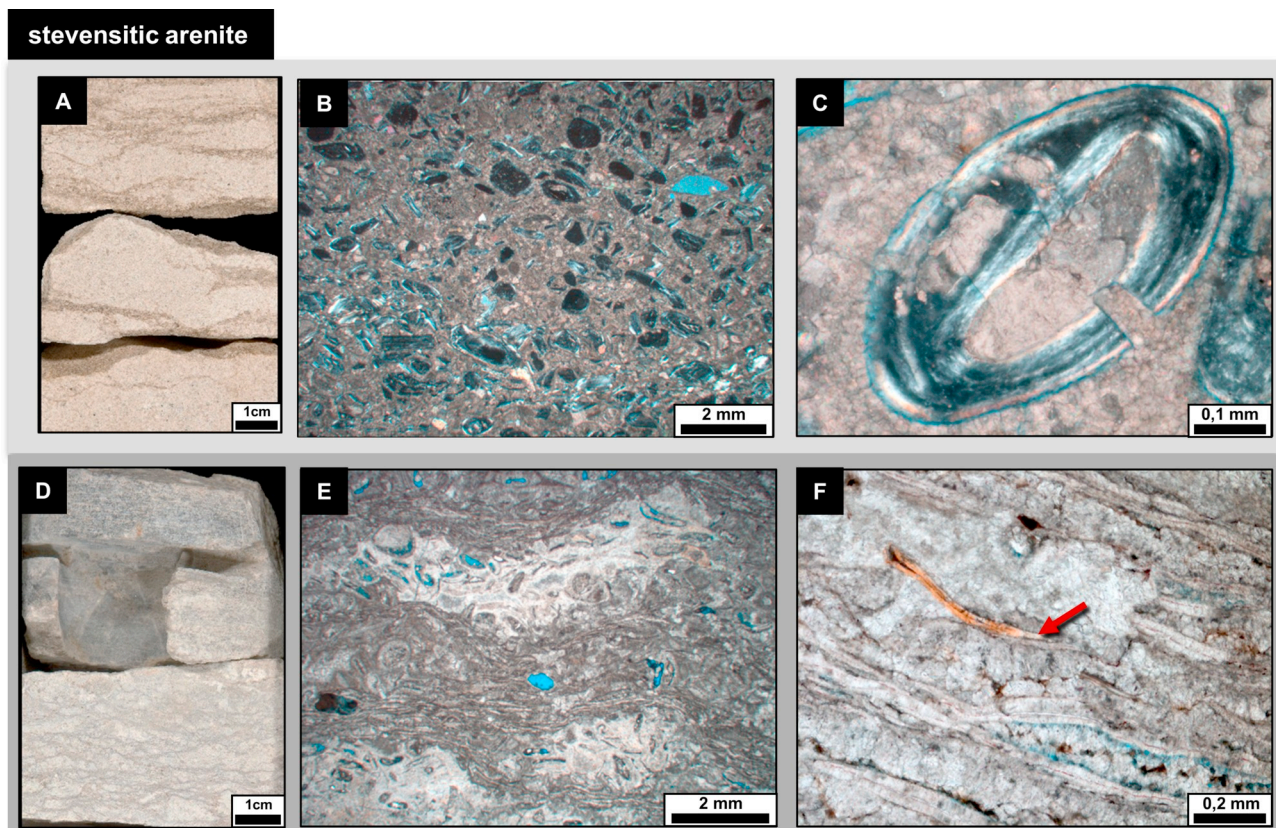


Fig. 19. Stevensitic arenite facies. A) Macroscopic aspect of the facies, WELL-1. B) Photomicrograph from WELL-1 (1,25X; uncrossed polarizers). C) Stevensitic ooid with regular and concentric lamination (WELL-1, XP). D) Macroscopic aspect of the facies, WELL-1. E) Photomicrograph from WELL-1 (uncrossed polarizers). F) Clay mineral laminae (red arrow) (WELL-1, uncrossed polarizers). (For interpretation of the references to colour in this figure legend, the reader is referred to the Web version of this article.)

grainstone (Rf and Gf) and, massive, poorly sorted, bivalve rudstone (Rm). This sequence occurs in both wells, usually with an erosive base, but is better expressed in WELL-2, where bed reached thickness of up to 15 m.

This succession is a record of the continuous reworking of the shells by waves and currents, above fair-weather wave base on the lake shoreface (Muniz, 2013). The energy to generate currents and waves in the lake could be induced by the wind, as observed in recent African lakes (Nutz et al. 2018; Schuster and Nutz, 2018). Reworked bioclastic bars are genetically related to the continuous high energy of water on structural highs producing also bioclastic calcarenite beaches (Carvalho et al. 2000).

5.1.3. Carbonate succession 3 – sublittoral lake carbonate deposit

Sublittoral carbonate deposits are distinguished by carbonate mud-supported rock (Mc), bivalve rudstone with micritic matrix (Ru), bivalve rudstone with a low degree of fragmentation (RI) and siliciclastic mudstone (Mg). Rarely, massive, poorly sorted, bivalve rudstone (Rm)

occurred intercalated with bivalve rudstone with micritic matrix. This succession was observed in both wells, especially within the basal interval of WELL-2.

This succession of facies is interpreted as a sublittoral deposit, where the energy was lower and carbonate mud could be deposited with less fragmented bioclasts intercalated with siliciclastic mudstone. Eventually, poorly sorted and massive rudstones suggest particles remobilization from structurally higher positions, by storms or tectonic destabilization.

5.1.4. Carbonate succession 4 – bioclastic deep lake fan

The bioclastic deep lake fan succession is composed of a large variety of facies, characterized by layers of massive, poorly sorted, bivalve rudstone (Rm), bivalve-gastropod rudstone (Rg) intercalated with mud-supported carbonate rock (Mc) and siliciclastic mudstone (Mg). This succession was distinguished in WELL-1 and WELL-2, with sharp base contacts.

Massive and poorly sorted deposits in deep environment can be

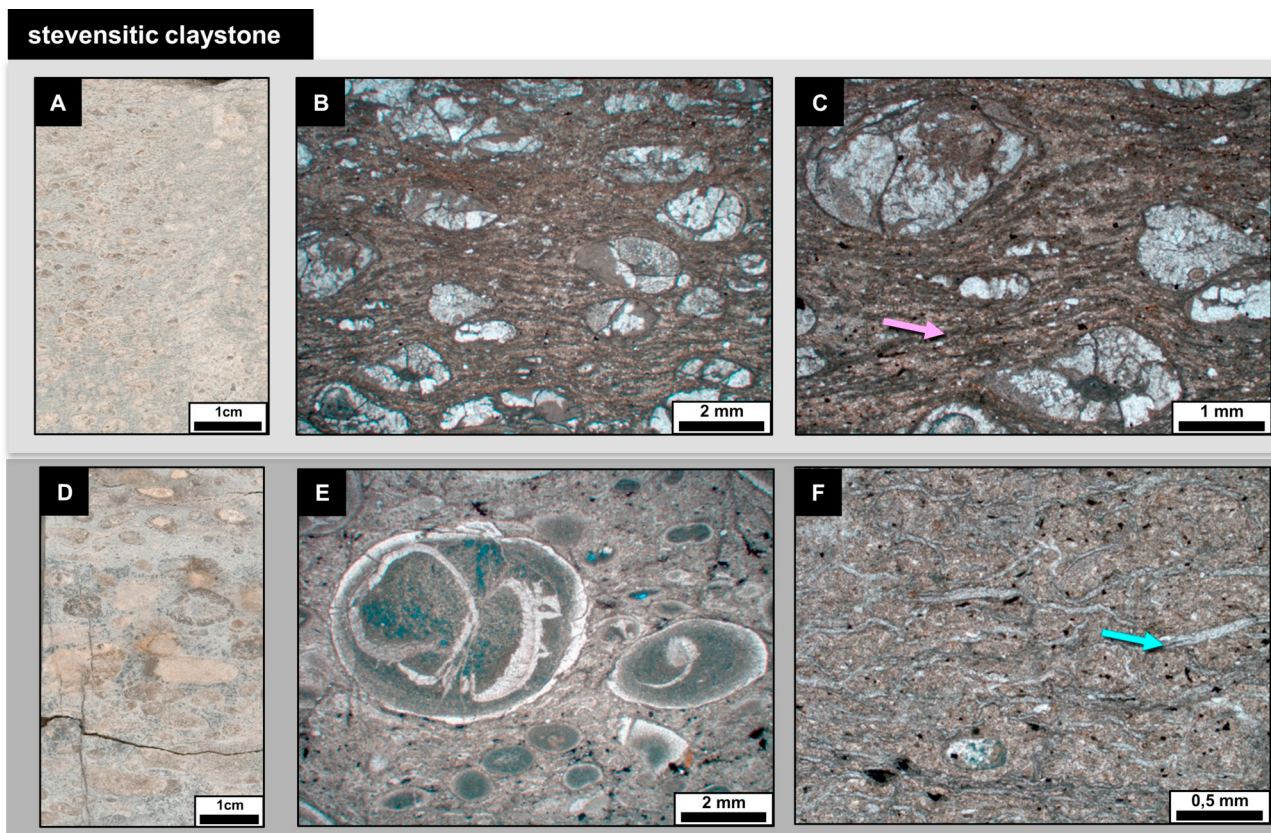


Fig. 20. Stevensitic claystone facies. A) Macroscopic aspect of the facies, WELL-1. B) Photomicrograph from WELL-1 (uncrossed polarizers). C) Clay mineral laminae dolomitized (pink arrow) (WELL-1, XP). D) Macroscopic aspect of the facies, WELL-1. with moldic pores (red arrow). E) Clay pisoids from WELL-1 (uncrossed polarizers). F) Clay mineral laminae detail (blue arrow) (WELL-1, uncrossed polarizers). (For interpretation of the references to colour in this figure legend, the reader is referred to the Web version of this article.)

generated by storms (Jahnert et al. 2012) or tectonically-driven gravitational flows (Goldberg et al. 2017). Based on the intercalation of episodic deposits, this facies succession is interpreted to have formed by destabilization of highs, and re-deposition intercalated with deep deposits (carbonate mud-supported rocks and siliciclastic mudstone) and hybrid arenites and conglomerates.

5.1.5. Hybrid succession – hybrid deep lake fan

Hybrid deep lake fan are composed by hybrid arenites and conglomerates (Ch) intercalated with bivalve rudstones and siliciclastic mudstone. This sequence was only observed in WELL-1.

The mixture of bioclasts with siliciclastic grains resulted from terrigenous clastic input to the lake by gravitational flows triggered by tectonics (Tavares et al. 2015) or storms (Carvalho et al. 2000). This kind of hybrid deposit could have deposited on the lake border associated to river mouths, as it is currently observed in Lake Tanganyika (Cohen, 1989a). The mixture of intrabasinal bioclastic and stevensitic

particles is related to remobilization of sediments by gravitational flows (Goldberg et al. 2017).

5.1.6. Magnesium clay succession

The magnesium clay succession is defined by stevensitic claystone (Cs), formed by in-situ clay precipitation, and stevensitic arenite (As), constituted by stevensitic ooids and peloids. Rarely, hybrid conglomerates and arenites are intercalated in this succession. This sequence was only found in WELL-1 as rare thin beds with less than 1 m thick.

Contemporaneous volcanism can provide magnesium to the water lake and favors stevensite precipitation (Abrahão and Warme, 1990). In Campos basin it is possible to have occurred exhumation of the mantle (Zalan et al., 2011), that might be an unusual and alternative source of Mg and SiO₂ required to precipitate Mg Silicates (Tosca and Wright, 2015). The formation of Mg-smectite demands high alkalinity, which is not ideal for bivalve proliferation (Rehim et al. 1986; Pozo and Casas, 1999; Herlinger et al. 2017). Environments with low energy protected

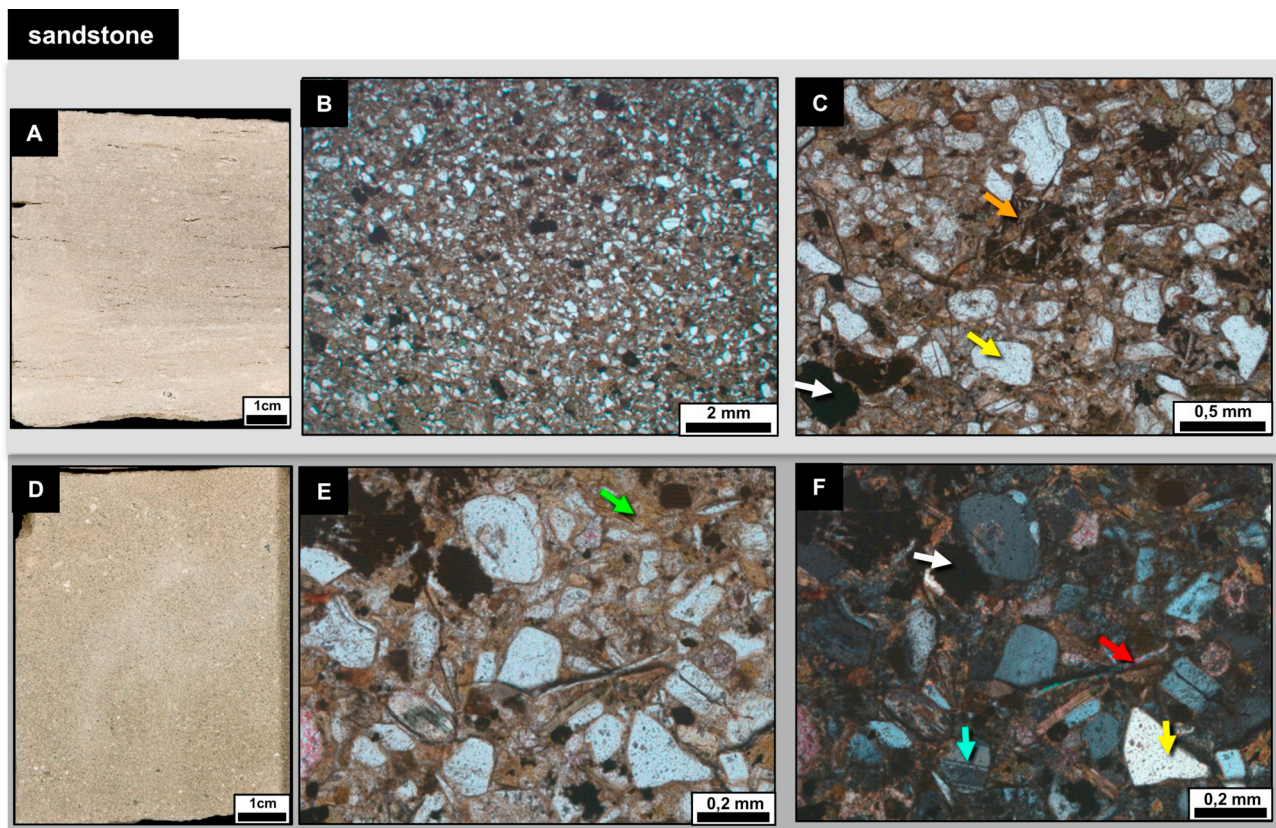


Fig. 21. Sandstone facies. A) Macroscopic aspect of the facies, WELL-1. B) Photomicrograph from WELL-1 (uncrossed polarizers). C – Quartz grain (yellow arrow), opaque mineral (white arrow) volcanic rock fragment (Orange arrow) (uncrossed polarizers). D)) Moderately sorted sandstone, WELL-1. E and F) Composition detail: quartz grain (yellow arrow), feldspar grain (blue arrow), mica grain (red arrow), opaque mineral (white arrow) and magnesium clay cement (E - uncrossed polarizers, F – XP). (For interpretation of the references to colour in this figure legend, the reader is referred to the Web version of this article.)

from big waves and currents were the sites where the clays generated (Herlinger et al. 2017).

5.1.7. Siliciclastic succession 1 - siliciclastic deep lake fan

Siliciclastic successions composed of fining and thinning upward layers of sandstones (S), with abrupt bases, intercalated with mudstones (Gs) are interpreted as turbidites. This succession was only observed in WELL-1.

Channelized turbiditic currents mobilize sediments to deeper portions of the lake due to heavily loaded flows coming from the fan deltas generated by episodic flooding events. (Tiercelin et al. 1994). The occurrence of alluvial fan and fan delta deposits resulted from the intense tectonic activity during the deposition of Coquinas Sequence in Campos Basin (Dias et al. 1988).

5.1.8. Siliciclastic succession 2 – deep lake siliciclastic deposit

The deep lake siliciclastic deposit succession is composed essentially by siliciclastic mudstones, which can reach thicknesses greater than 5 m

and occur associated with hybrid conglomerates and sandstones (Ch and Ah), and massive, poorly sorted, bivalve rudstone (Rm). This succession were recognized in both wells, but it is thicker in WELL-1.

This deposit was formed in the central and deeper portions of the lake (Bertani and Carozzi, 1985a; Dias et al. 1988; Abrahão and Warme, 1990; Carvalho et al. 2000). This facies succession is interpreted as formed by the decantation of the finest siliciclastic particles brought into the lake by hypopycnal flows at the moments of floodings and wetland dominance, during transgressions and higher water levels. Conglomerates, arenites and rudstones were deposited gravitationally by episodic storms, floodings or tectonics. Occasionally, the lake level could have been so low that the mudstone was reddened by oxidation (Abrahão and Warme, 1990).

The percentage of facies successions in each studied well are represented in Fig. 25. A detailed representation of facies succession (FS) stacking model revealed the important differences between the two wells pointing the offshore well as composed basically of carbonates whilst the proximal well presents a mixing of FS (Fig. 26). WELL-1

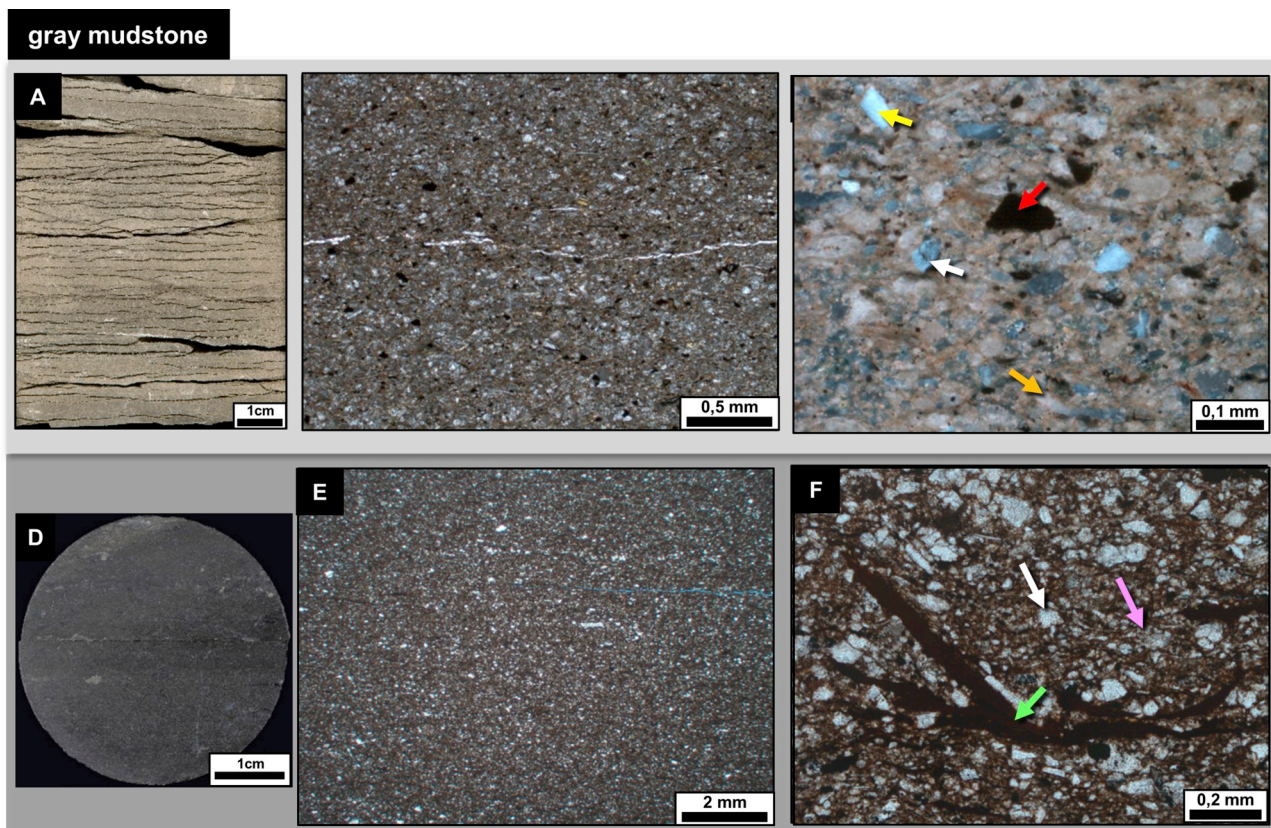


Fig. 22. Gray mudstone facies. A) Macroscopic aspect of a laminated gray mudstone WELL-1. B) Photomicrograph detail from WELL-1 (uncrossed polarizers). C) Composition detail: quartz grain (yellow arrow), feldspar grain (white arrow), opaque mineral (red arrow) (uncrossed polarizers, with alizarin staining). D) Macroscopic aspect of a sidewall core, WELL-2. E) Photomicrograph from WELL-2 (uncrossed polarizers). F) Composition detail: feldspar grain (white arrow), vertebrate fragment (green yellow) and dolomite cement (pink arrow) (WELL-2, uncrossed polarizers). (For interpretation of the references to colour in this figure legend, the reader is referred to the Web version of this article.)

presented a more diverse mixing of facies successions, represented by carbonate, hybrid, clay and siliciclastic successions. Successions of hybrid and siliciclastic lake fans, and deep lake mudstones dominate, as well as bioclastic bars and bioclastic lake fans. WELL-2 is composed by carbonate successions, mainly bars, and secondarily, reworked bars predominate with no magnesium clay succession, neither hybrid and siliciclastic fan succession.

5.2. Depositional model

Based on the facies stacking pattern analysis, distinct conceptual depositional models can be suggested for each geological setting during the lower Aptian. A hybrid sedimentary record was sampled in WELL-1, with carbonate (predominantly bivalve rudstones), interlayered with siliciclastic rocks (mudstones and sandstones). These sediments were interpreted as deposited on a lake ramp, close to the rift margins, with alternation of carbonate and siliciclastic deposits, typical of the hybrid geological setting. On the other hand, the sedimentary record of WELL-

2 is basically composed of carbonate rocks, predominantly massive, poorly sorted, bivalve rudstones (Rm) and organized bivalve rudstones (Ro). These sediments were interpreted as deposited on an isolated bioclastic carbonate high located on Campos Basin External High, without significant terrigenous contribution.

5.2.1. Hybrid ramp in rift setting

The hybrid rift setting is characterized by the intercalation of non-carbonate and carbonate rocks (Fig. 27). The non-carbonate rocks are hybrid conglomerates and arenites, stevensitic arenite and claystone, sandstone and mudstone. The carbonate rocks are mainly massive, poorly sorted, bivalve rudstones and, secondarily, there are broken and rounded shells rudstones and grainstones, organized bivalve rudstones and bivalve rudstones with whole shells.

When fresh-water conditions are prevailed in the lake the bivalve productivity increases despite that some species live in saline conditions. These bioclasts are eventually remobilized to the lake borders forming bars, which can be reworked by longshore currents and waves.

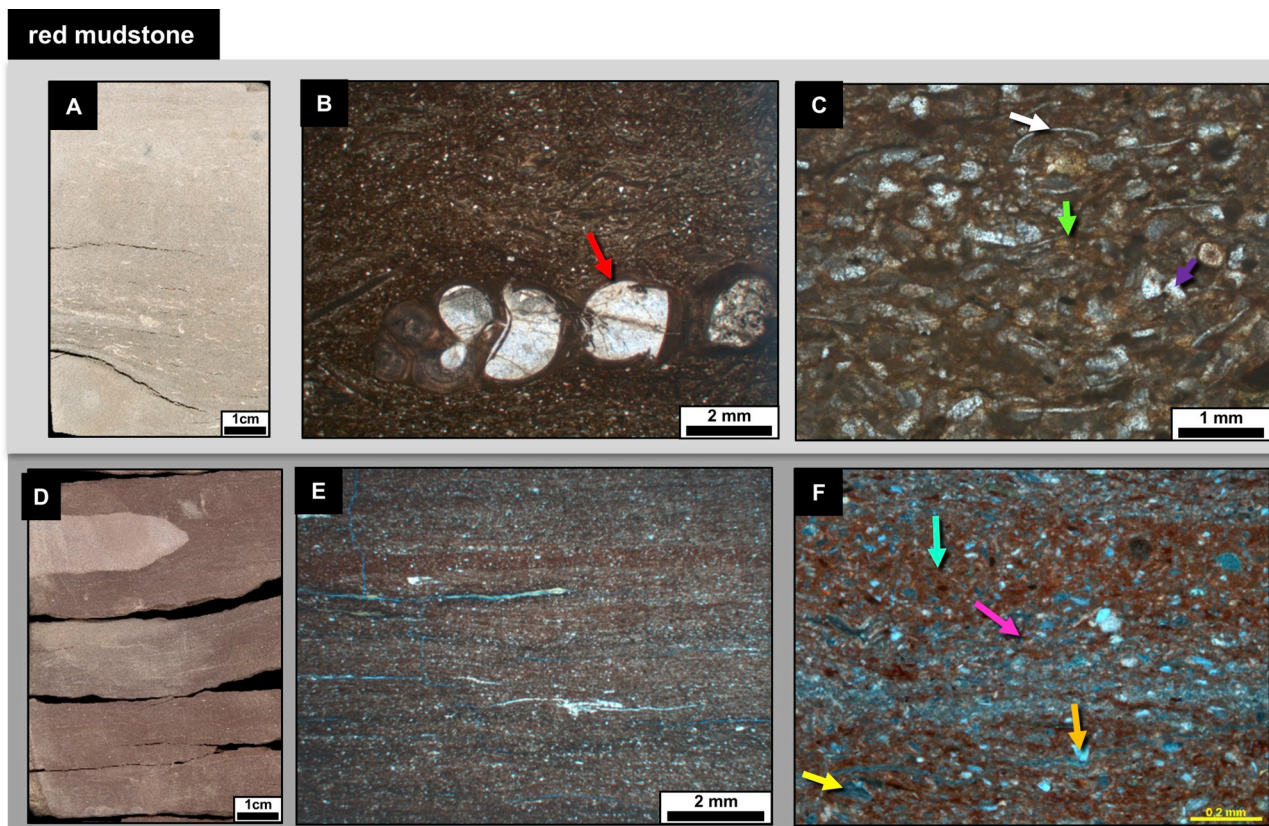


Fig. 23. Red mudstone facies. A) Macroscopic aspect of the facies, WELL-1. B) Red mudstone with gastropod (red arrow) (uncrossed polarizers). C) Composition detail: quartz grain (pink arrow), disarticulated ostracod (yellow arrow) and clay matrix (blue arrow) (uncrossed polarizers, with alizarin staining). D) Macroscopic aspect of the a red mudstone with an incipient lamination, WELL-1. E) Incipient lamination (1,25X; uncrossed polarizers). F) D – Red mudstone composition: plagioclase (yellow arrow), quartz (orange arrow) and mica (pink arrow) with magnesium clay matrix (blue arrow) (WELL-1, XP). (For interpretation of the references to colour in this figure legend, the reader is referred to the Web version of this article.)

Moreover, storms may have generated washover fan deposits on the structural highs, in the backshore, and also remobilized sediments to the lows with gravitational flows forming bioclastic deep lake deposits. Sediments may also have been redeposited in the lows by gravitational flows triggered by tectonic destabilization of the structural highs. In the case of re-sedimentation to a deeper environment, remobilized sediments were intercalated with mudstones and carbonate mud supported rocks.

The periods with higher alkalinity of the water lake, which may be associated to contemporaneous volcanism, favored magnesium-clay occurrence once the strong input of CO_2 in the lake water contributed to the biogenic production of HCO_3^- and CO_3^{2-} transforming environments in alkaline. With the disponibility of high contents of Mg and Si the lakes were able to develop extensive deposits of magnesium clays. Some water agitation by waves or currents can form stevensitic grain

coatings typical of stevensitic arenites.

Terrigenous influx in the depositional ramp could have been related to alluvial fans or flood-induced hyperpycnal flows that trigger turbiditic currents. The sandstones are deep lake fans deposited by episodic turbidite currents. Hybrid deposits formed as mixtures of bioclasts, siliciclastic grains, and stevensitic ooids or peloids in variable proportions. These deposits originated by storms and gravitational flows, which combine particles of different origins, as hybrid deep lake fans.

Hybrid ramps in rift setting were described in lacustrine coquinas of lower Cretaceous of Sergipe-Alagoas Basin (Tavares et al. 2015; Chinellatto et al. 2018) and in modern East African rift lakes (Cohen, 1989a; Tiercelin et al. 1994). In Lake Tanganyika, in the East African rift system, there are lag deposits of coquinas with gastropods, ostracods and bivalves mixed with quartz and feldspar grains in the littoral platform associated with ramped sides of half-grabens (Tiercelin

Table 2
Facies succession of Coqueiros Formation, based on the studied wells.

Nº	Acronym	Facies Succession	Related Facies	Occurrence	Interpretation
CARBONATE SUCCESSION					
1	BAR	Bioclastic bar	Rm	WELL-1 and WELL-2	High energy environments from storms or tsunamis, with continuous subsidence.
2	BARr	Reworked bioclastic bar	Ro, Rf, Rg	WELL-1 and WELL-2	Continuous reworking of the shells by waves and currents, above fairweather wave base.
3	SLC	Sublittoral lake carbonate deposit	Mc, Ru, Rw, Mg	WELL-1 and WELL-2	Low energy environments, in protected or relatively deep areas, with micrite decantation and bivalve shells non-fragmented.
4	BDF	Bioclastic deep lake fan	Rm, Ah, Ch, Ms, Ms, Rg	WELL-1 and WELL-2	Event deposits, formed by highs destabilization and re-sedimented by storms or tectonically-driven gravitational flows.
-	HDF	Hybrid deep lake fan	Ah, Ch, Mg	WELL-1	Event deposits, formed by highs destabilization and re-sedimentation. Siliciclastic grains are related to continental contribution, by tectonic pulses, floods, or storm-induced currents. The mixture of bioclastic with intrabacinal stevensitic particles are related to storms or tectonically-driven gravitational flows.
-	MCS	Magnesium clay succession	As, Cs	WELL-1	Precipitation in more alkaline conditions than the ideal condition for bivalve proliferation in lacustrine or palustre environment, with some agitation by waves or currents. Contemporaneous volcanism can be the source of magnesium to the water lake.
M. CLAY					
1	SDF	Siliciclastic deep lake fan	S, Mg	WELL-1	Episodic turbidity currents that advance from the continent to the basin during floods.
2	DLS	Deep lake siliciclastic deposit	Mg, Ah, Ch, Rm	WELL-1 and WELL-2	Siliciclastic decantation from continent, with low energy during high lake phases.

et al. 1994). In large rift lakes, as Tanganyika, asymmetry exerts a strong control on facies patterns. Deltas and fan deltas introduce abundant sediment to the shoreline that is reworked by waves and longshore currents (Soreghan and Cohen, 1996).

5.2.2. Isolated bioclastic high in rift setting

According to the sedimentary assembly in WELL-2, an isolated bioclastic high depositional setting was drilled, characterized principally by, massive, poorly sorted, bivalve rudstone, organized bivalve rudstone, broken and rounded shells rudstones and grainstones, and bivalve rudstone with whole shells (Fig. 28). Locally, there are ostracod-bivalve packstone, bivalve rudstone with micritic matrix, mud-supported carbonate rock, and gray mudstone.

At this isolated high the conditions were appropriated for bivalves to live and proliferate, for long periods without climatic, biophysical or biochemical changes and significant siliciclastic input. In rift settings with continuous generation of accommodation space, the occurrence of amalgamated layer of massive, poorly sorted, bivalve rudstones with no intercalated deep lake sediments as mudstones give support to the idea that these deposits are nearshore bars formed by storms. Eventually, bioclastic bars are reworked by current and waves, and igneous basement may be exposed, forming fragmented and organized bioclastic bivalves, with important coquina intraclasts and volcanic rock fragments.

Inside low energy conditions the predominant sedimentary sequence were composed of mud-supported carbonate rock and bivalve rudstone with micritic matrix. In relative deeper portions, siliciclastic mudstones are intercalated with massive rudstones deposited by storms or tectonically driven gravitational flows. In the bioclastic isolated high few hybrid rocks with bivalve bioclasts and volcanic fragments were described. The siliciclastic grains observed are silt-sized quartz, feldspar and mica grains, related to terrigenous hypopycnal plumes, which developed deep lake siliciclastic deposits.

Bioclastic carbonate sequences, without terrigenous components are peculiar and diagnostic of isolated bioclastic highs in rift settings as observed in Mero and Buzios oil fields in the Pre-Salt, lower Cretaceous, in Santos Basin (Petersohn and Abelha, 2013; Carlotto et al. 2017).

5.2.3. Depositional model for the bioclastic deposits

A conceptual depositional model was proposed based on the characteristics of the two geological settings represented by the sedimentary sequence described and interpreted from WELL-1 and WELL-2 (Fig. 29). The schematic diagram block was elaborated using the structural framework of the Campos Basin (Rangel and Martins, 1998) to rebuild the approximate paleogeography.

The carbonate sedimentation during the lower Aptian, occurred in a rift lake, with high bivalve productivity associated with basement highs providing ideal conditions for the development of bioclastic bars, which were accumulated by storms and were reworked by fairweather waves and longshore currents. The structural highs were eventually exposed and eroded during lake levels oscillations. Close to the lake border, over the Badejo High, sandstones were deposited by turbidite currents on a carbonate ramp affected by intense tectonic activity and submitted to storms action. Locally, the changes in lake chemistry favored the precipitation of magnesium rich clay minerals. Probably, this Mg enrichment was related to arid conditions and simultaneous volcanism. Episodically, siliciclastic, carbonate and stevensitic grains were mixed by re-sedimentation in deeper environment by storms and tectonically driven gravitational flows, forming hybrid deposits.

Far from the rift border, bioclastic sedimentation predominated on isolated highs on the External High. Siliciclastic mudstones were deposited in structural lows by hypopycnal flows during flooding events. In the structural lows, low energy environment, mud supported carbonates dominated. In basin grabens, carbonate mudstones interlayer with reworked sediments from structural highs.

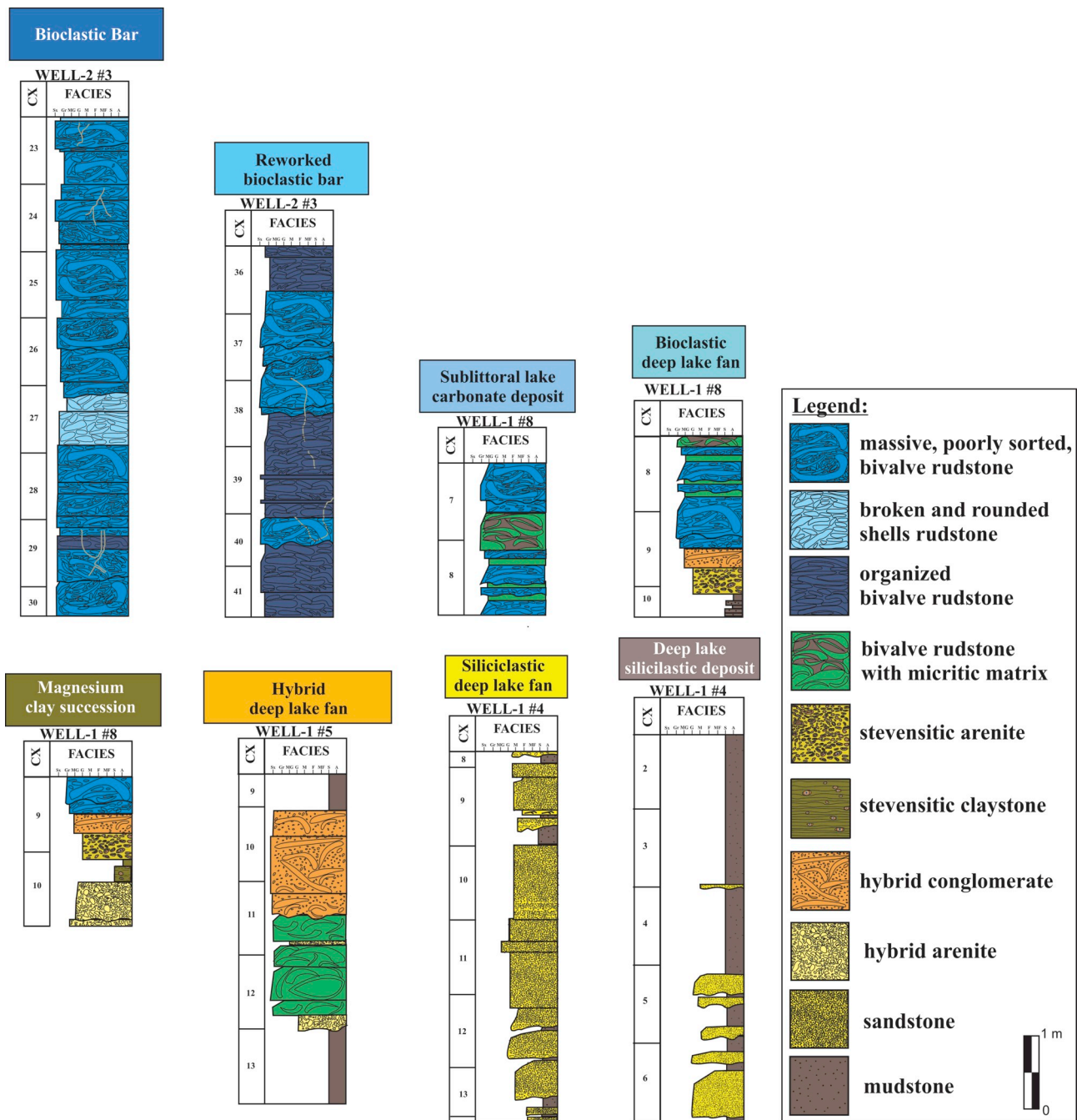


Fig. 24. Facies succession interpreted based on macroscopic and microscopic description of WELL-1 and WELL-2.

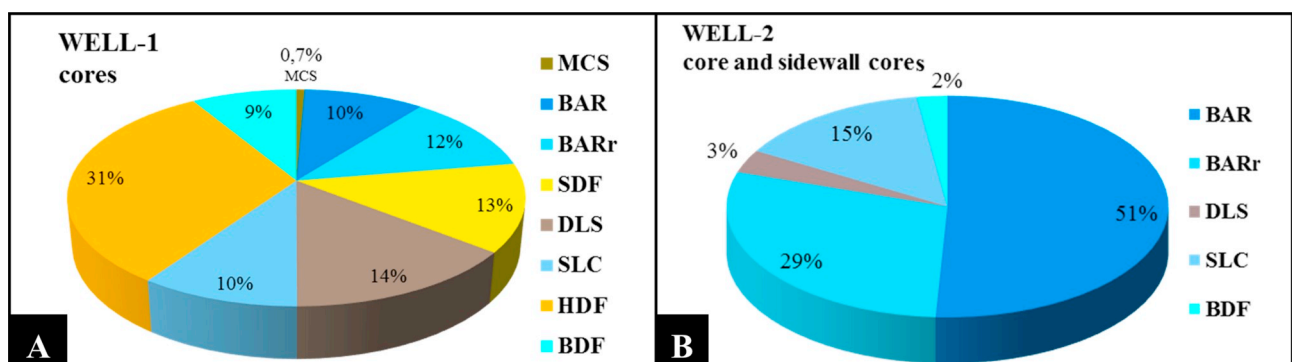


Fig. 25. Facies successions occurrence in WELL-1 core, and core and sidewall cores of WELL-2. A) In WELL-1, the most common facies successions are hybrid deep lake fan (HDF), besides siliciclastic deep lake fan (SDF), deep siliciclastic lake (DLS) and bioclastic bar successions (BAR). B) In WELL-2, the most common facies successions are the bioclastic bars (BAR). For facies succession abbreviation, see Table 2.

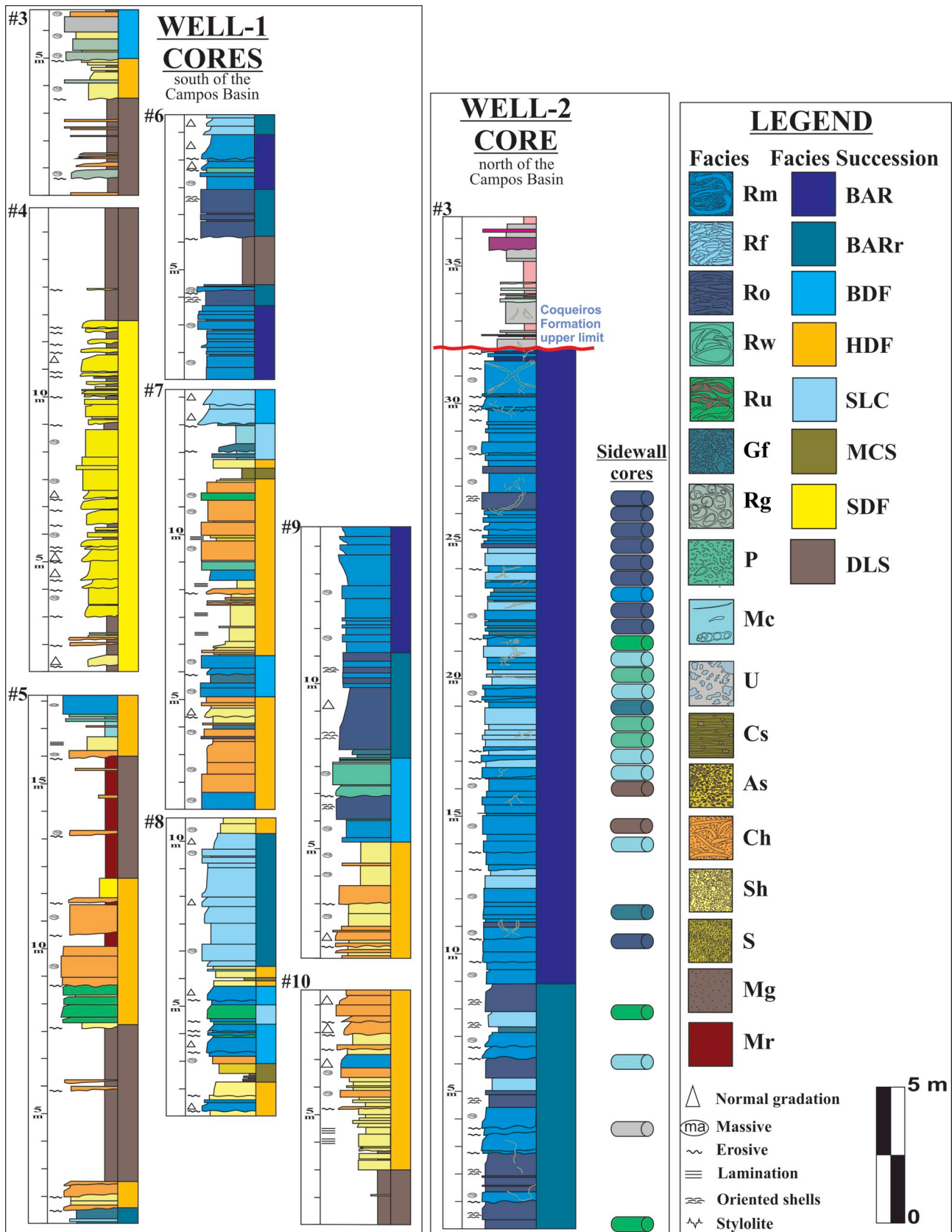


Fig. 26. Core and sidewall cores descriptions and facies successions interpreted. For samples position, see Fig. 3. For facies abbreviation, see Table 1, and for facies succession abbreviation, see Table 2.

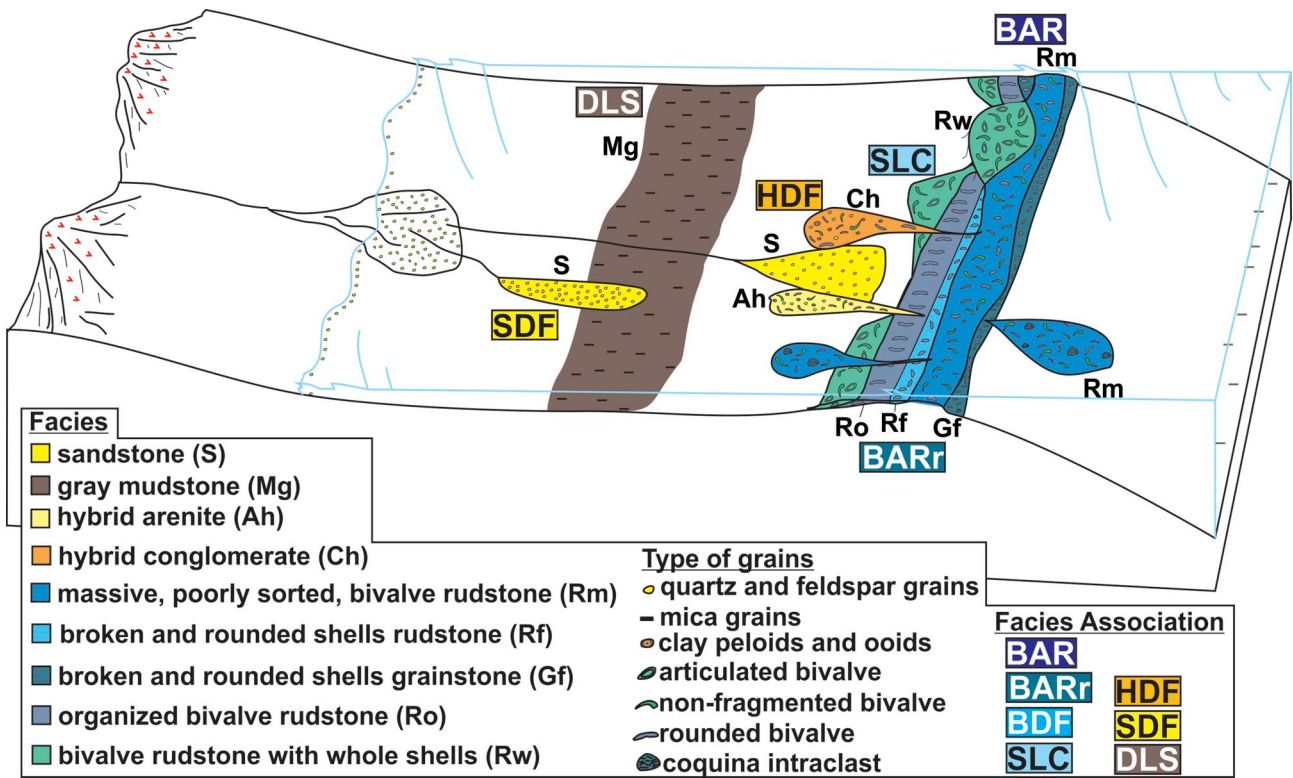


Fig. 27. Depositional model for a hybrid ramp, based on WELL-1 facies and facies successions. The succession of magnesium clay mineral are not represented because it is related to major changes in water biochemistry, that diffculted the establishment of the stacking patterns. For facies succession abbreviations, see Table 2.

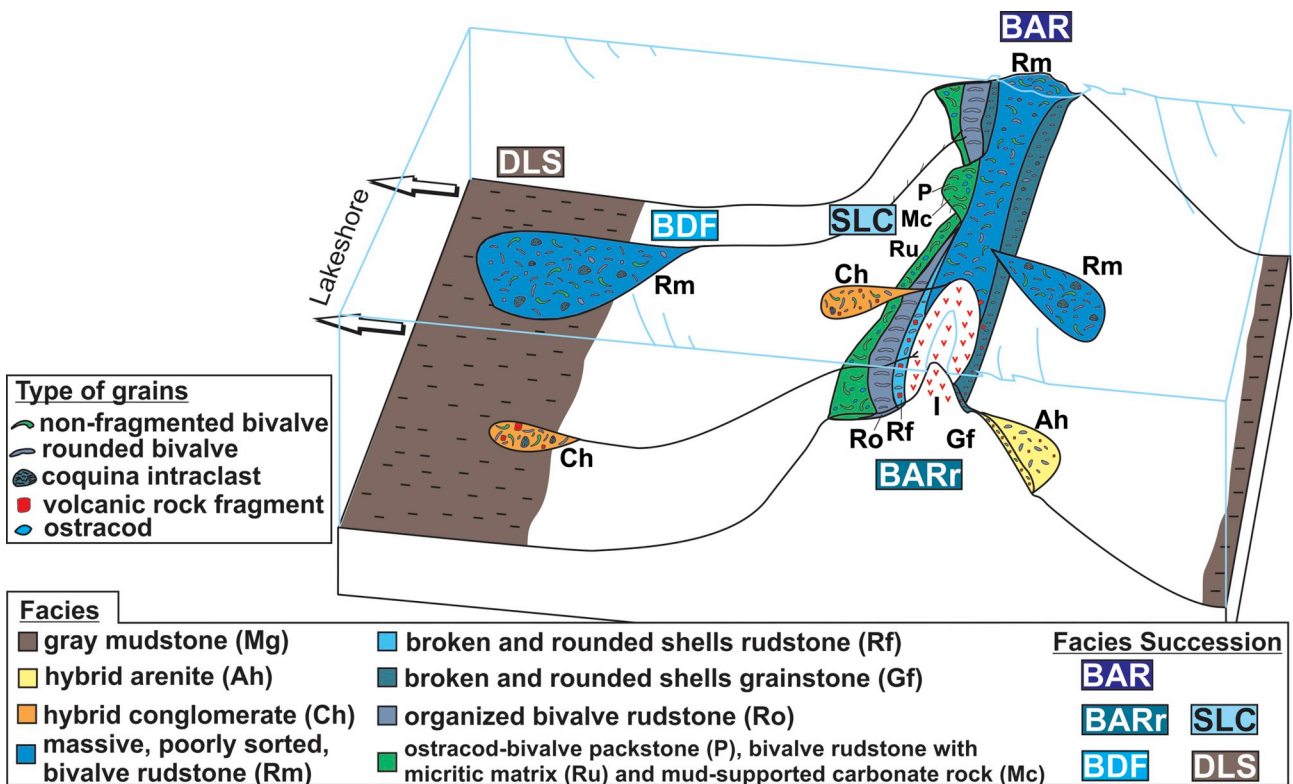


Fig. 28. Depositional model for an isolated bioclastic high, based on WELL-2 facies and facies successions. The "I" letter represents igneous rocks. Hybrids successions are not significant on the isolated bioclastic highs. For facies succession abbreviations, see Table 2.

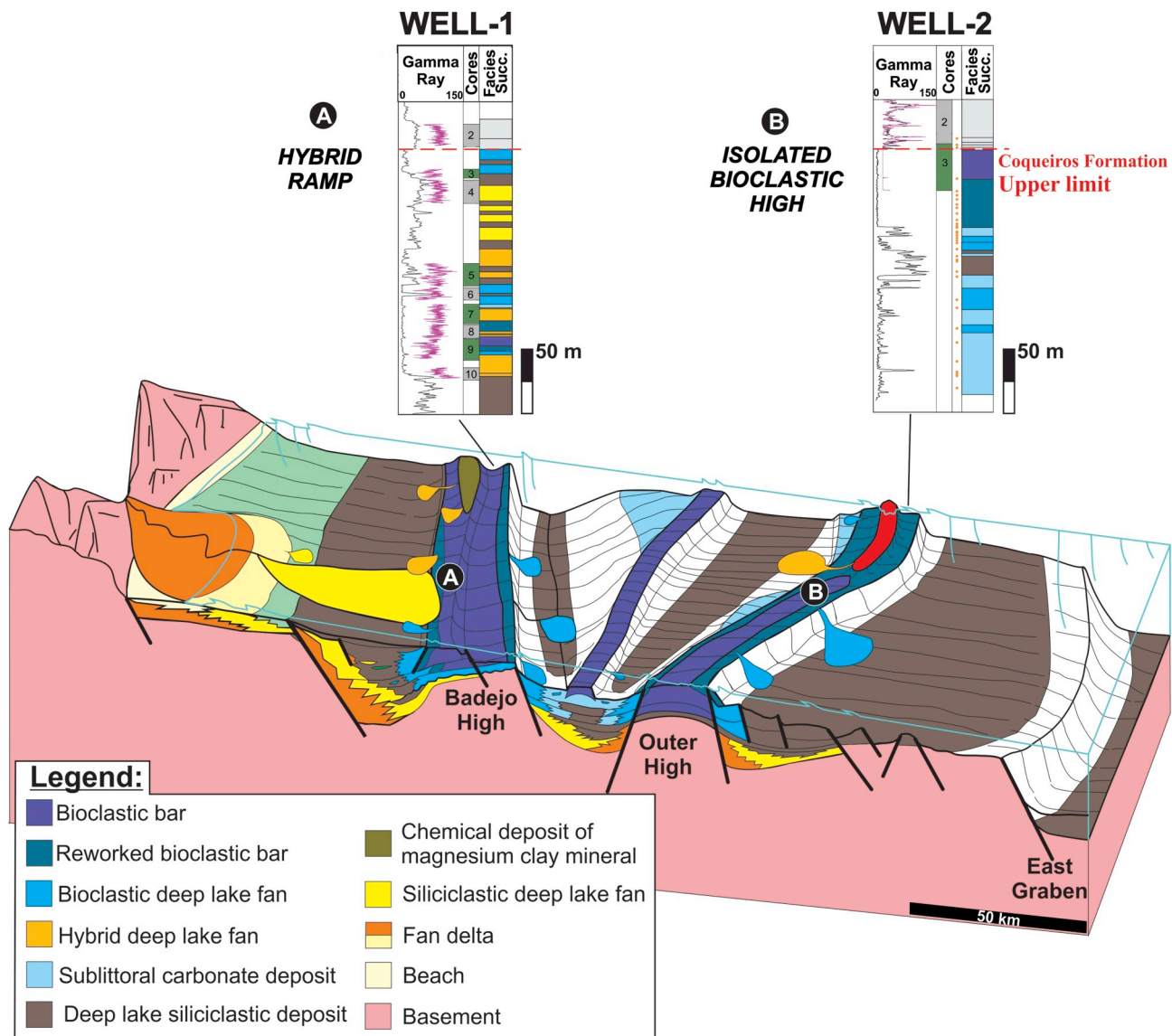


Fig. 29. Proposed depositional model of lower Aptian, rift section of the Campos Basin, based on sedimentological analysis of wells 1 and 2 and the structural framework inherited from basement of Campos Basin. The (A) correspond to WELL-1 located in a hybrid ramp, and (B), at the External High, WELL-2 projection, drilled over a bioclastic isolated high.

5.2.4. Exploratory implications

The facies with the best reservoir quality is the massive, poorly sorted, bivalve rudstone that formed over structural highs, as nearshore bars deposited by storms and reworked by fair-weather waves and currents, or in deeper portions as re-sedimented carbonate deposited by gravitational flows.

Because of the high concentration of bioclasts, it is possible that in structural lows, exploratory wells may find thick coquina deposits. These deposits would have formed as distal tempestites or tectonic related gravitational flows. In lake Tanganyika, there are sublacustrine channels that feed deep-water environments coarse-grained, bioclastic material (Soreghan and Cohen, 1996). If these rocks are essentially composed of bivalve shells, they may have high primary porosity preserved as well as high secondary porosity generated by dissolution. These reservoirs are intercalated with low permeability facies, which may behave as permeability barriers. However, if the deposits have hybrid composition, with siliciclastic and/or stensentic grains, intense processes of compaction and dolomite and calcite cementation can dramatically decrease the reservoir permo-porosity.

The recent discovered Pre-Salt fields in on the External High of

Santos Basin presented oil accumulation in lower Aptian coquinas deposited on basement structural highs of Santos Basin (Carminatti et al. 2008; Petersohn and Abelha, 2013; Abelha, 2015; Carlotto et al. 2017). These bivalve coquinas contain minor quantities of intraclasts, hybrid composition, siliciclastic sediments and pelitic layers.

Based on the similarities between the Pre-Salt coquina reservoirs located on the External High of Santos Basin and those located on the External High of Campos Basin exploratory challenges may partially be addressed and the experience registered by this research help to improve the exploratory drillings looking for new discoveries. Therefore, exploratory campaigns can be successful in bioclastic reservoirs generated in structural highs, preferentially distant from the lake borders with low terrigenous influx.

6. Conclusions

A depositional model for the coquinas sequence of Campos Basin emerged from a detail facies and facies succession analyses. In this model, bioclastic deposits are related to basement structural highs, which can be interlayered with siliciclastic deposits produced by

terrigenous influx by gravitational flows produced by floods or tectonic events.

In this study, due to the detailed analysis performed in microscopic scale, not only particles of bivalves were identified in the coquinas but also ostracods, gastropods, coquina intraclasts, volcanic rock fragments, and stevensite ooids and peloids.

The sedimentary record of the studied wells comprises carbonate, hybrid, talc-stevensite and siliciclastic rocks. Using composition, texture and taphonomic criteria, 17 facies were defined.

The facies stacking patterns observed in the two geological settings characterized eight facies successions. The hybrid carbonate ramp revealed strong terrigenous influence and large variation of the lake water chemistry, located in Badejo High, it is characterized by carbonate, clay, siliciclastic and hybrid successions. On the other hand, the isolated bioclastic high located on External High contains basically carbonate successions, except for the local occurrence of siliciclastic from deep lake, produced by regional flooding.

Therefore, during the lower Aptian in Campos Basin, carbonate sedimentation occurred in a rift context, with robust bioclastic productivity on basement highs. In structures adjacent to the lake border, terrigenous influence is higher, due to structural high gradients, forming hybrid and siliciclastic deposits, interlayered with carbonate rocks. Isolated highs distant from the lake border were characterized as excellent exploratory targets for coquinas reservoirs, because of the high water energy that moved away the fine sediment particles and due to the low terrigenous influence.

Episodic storms or tectonically driven waves could have formed the nearshore bars and the deep-water gravitational flow deposits. Fairweather waves and currents then reworked these bars.

Bioclastic bars characterized by thick successions of massive, poorly sorted, bivalve rudstones are the thickest and best reservoirs.

The predominant bivalve enriched facies succession described in the WELL-2 demonstrated how important was the reconnaissance of the paleo-environment for any exploratory campaign. Structural isolated highs located far from the proximal rift border are best targets, once they are protected from the terrigenous influx promoted by hyper and hypopycnal flows. The depositional model constructed for each well demonstrated the differences between proximal and distal facies successions located at proximal and distal structural highs.

Acknowledgements

The authors acknowledge the Brazilian National Petroleum Agency (ANP) for data liberation and Petrobras for the access to samples and well logs, analysis support, and permission to publish this work. The authors also thank Caroline de Oliveira Nardi Leite and Luci Maria Arienti for suggestions of improvement, and Ricardo Likawka for exploratory wells recommendation. This paper benefited greatly by revisions from Reviewer 1 and Reviewer 2.

Appendix A. Supplementary data

Supplementary data to this article can be found online at <https://doi.org/10.1016/j.jsames.2019.102254>.

References

- Abelha, M., 2015. Brazilian Carbonate Oil Fields: A Perspective. Brazilian Petroleum Conference - Carbonates: From Genesis to Production - Rio de Janeiro/Brazil.
- Abrahão, D., Warme, J.E., 1990. Lacustrine and associated deposits in a rifted continental margin-lower cretaceous lagoa feia formation, Campos basin, offshore Brazil. In: Katz, B.J. (Ed.), *Lacustrine Basin Exploration: Case Studies and Modern Analogs*. AAPG Memoir 50, pp. 287–305.
- Armelenti, G., Goldberg, K., Kuchle, J., De Ros, L.F., 2016. Deposition, diagenesis and reservoir potential of non-carbonate sedimentary rocks from the rift section of Campos Basin, Brazil. *Petrol. Geosci.* 22 (3), 223–239.
- Bates, C.C., 1953. Rational theory of delta formation. *AAPG (Am. Assoc. Pet. Geol.) Bull.* 37, 219–2162.
- Baumann, A., Forstner, U., Rohde, R., 1975. Lake Shala—water chemistry, mineralogy, and geochemistry of sediments in an Ethiopian rift lake. *Geol. Rundsch.* 64, 593–609.
- Bertani, R.T., 1984. Microfacies, Depositional Models and Diagenesis of Lagoa Feia Formation (Lower Cretaceous), Campos Basin, Offshore Brazil. PhD. thesis. University of Illinois at Urbana-Champaign, pp. 199.
- Bertani, R.T., Carozzi, A.V., 1985a. Lagoa feia formation (lower cretaceous), Campos basin, offshore Brazil: rift valley stage lacustrine carbonate reservoirs — I. *J. Pet. Geol.* 8 (1), 37–58.
- Bertani, R.T., Carozzi, A.V., 1985b. Lagoa feia formation (lower cretaceous), Campos basin, offshore Brazil: rift valley stage lacustrine carbonate reservoirs — II. *J. Pet. Geol.* 8 (2), 199–220.
- Brown, G., Brindley, G.W., 1980. X-Ray diffraction procedure for clay mineral identifications. In: Brindley, G.W., Brown, G. (Eds.), *Crystal Structures of Clay Minerals and Their X-Ray Identification*. Londres Mineralogical Society, pp. 305–359.
- Bryant, E.A., Young, R.W., Price, D.M., 1992. Evidence of tsunami sedimentation on the southeastern coast of Australia. *J. Geol.* 100, 753–765.
- Bruhn, C.H.L., Gomes, J.A.T., Lucchese, C.D., Johann, P.R.S., 2003. Campos basin: reservoir characterization and management – historical overview and future challenges. In: *OTC 15220. Offshore Technology Conference*, Houston, Texas, pp. 14pp.
- Bustillo, M.A., Arribas, M.E., Bustillo, M., 2002. Dolomitization and silicification in low-energy lacustrine carbonates, Paleogene, Madrid Basin, Spain. *Sediment. Geol.* 151 (1–2), 107–126.
- Bustillo, M.A., 2010. Silicification of continental carbonates. In: Alonso-Zarza, A.M., Tanner, L.H. (Eds.), *Carbonates in Continental Settings: Geochemistry, Diagenesis and Applications*. Developments in Sedimentology. vol. 62, pp. 153–174.
- Bustillo, M.A., Armenteros, I., Huerta, P., 2017. Dolomitization, gypsum calcitization and silicification in carbonate–evaporite shallow lacustrine deposits. *Sedimentology* 64, 1147–1172.
- Carlotto, M.A., Da Silva, R.C.B., Yamato, A.A., 2017. Libra: a newborn giant in the Brazilian presalt province. In: Merrill, R.K., Sternbach, C.A. (Eds.), *Giant Fields of the Decade 2000–2010*. vol. 113. AAPG Memoir, pp. 165–176.
- Carminatti, M., Wolff, B., Gamboa, L.A.P., 2008. *New Exploratory Frontiers in Brazil: 19th. World Petroleum Congress*, Madrid, Spain 2008.
- Carvalho, M.D., Praca, U.M., Telles, A.C.S., 2000. Bioclastic carbonate lacustrine facies molds in the Campos basin (lower cretaceous), Brazil. In: Gierlowski-kordesch, E.H., Kelts, K.R. (Eds.), *Lake Basins through Space and Time*. Tulsa: AAPG. AAPG Studies in Geology. vol. 46, pp. 245–256.
- Chang, H.K., Kowsmann, R.O., Figueiredo, A.M.F., Bender, A.A., 1992. Tectonics and stratigraphy of the East Brazil Rift system: an overview. *Tectonophysics* 213, 97–138.
- Chinelatto, G.F., Vidal, A.C., Kuroda, M.C., Basilici, G.B., 2018. A taphofacies model for coquina sedimentation in lakes (Lower Cretaceous, Morro do Chaves Formation, NE Brazil). *Cretac. Res.* 85, 1–19.
- Cohen, A.S., 1989a. Facies relationships and sedimentation in large rift lakes and implications for hydrocarbon exploration: examples from lakes Turkana and Tanganyika. *Palaeogeogr. Palaeoclimatol. Palaeoecol.* 70, 65–80.
- Cohen, A.S., 1989b. The taphonomy of gastropod shell accumulations in large lakes: an example from Lake Tanganyika. *Paleobiology* 15, 26–45.
- Conceição, J.C.J., Zalan, P.V., Wolff, S., 1988. Mecanismo, evolução e cronologia do rift Sul-Atlântico. *Bol. Geociencias Petrobras* 2, 255–265.
- Dale, C.T., Lopes, J.R., Abilio, S., 1992. Takula Oil Field and the Greater Takula Area, Cabinda, Angola. In: Halbouty, M.T. (Ed.), *Giant Oil and Gas Fields of the Decade 1978–1988*. AAPG Memoir 54. AAPG, Tulsa, Oklahoma, USA, pp. 197–215.
- Dawson, A.G., Stewart, I., 2007. Tsunami deposits in the geological record. *Sediment. Geol.* 200, 166–183.
- Dehler, N.M., Magnavita, L.P., Gomes, L.C., Rigoti, C.A., Oliveira, J.A.B., Sant’anna, M.V., Costa, F.G.D., 2016. The ‘Helmut’ geophysical anomaly: a regional left-lateral transtensional shear zone system connecting Santos and Campos basins, southeastern Brazil. *Mar. Pet. Geol.* 72, 412–422.
- Dias, J.L., Oliveira, J.Q., Vieira, J.C., 1988. Sedimentological and stratigraphic analysis of the lagoa feia formation, rift phase of Campos basin, offshore Brazil. *Rev. Bras. Geociencias* 18 (3), 252–260.
- Dias, J.L., 2005. Stratigraphy, sedimentology and volcanism of the Lower Cretaceous phase along eastern Brazilian continental margin. In: 14th International Congress of the IAS, 2005, Recife. *Annals. Recife*, pp. 1–2.
- Dias, J.L., Scarton, J.C., Esteves, F.R., Carminatti, M., Guardado, L.R., 1990. Aspectos da evolução tectono-sedimentar e a ocorrência de hidrocarbonetos na Bacia de Campos. In: Gabaglia, G.P.R., Milani, E.J., Origen, E., *Evolução, de Bacias, Sedimentares, Petrobras* (Eds.), Rio de Janeiro, pp. 333–360.
- Dunham, R.J., 1962. Classification of carbonate rocks according to depositional texture. In: Ham, W.E. (Ed.), *Classification of Carbonate Rocks*. American Association of Petroleum Geologists Memoir, pp. 108–121.
- Embry, A.F., Klovan, J.E., 1971. A late devonian reef tract on northeastern banks Island, NWT. *Canadian Petroleum Geology Bulletin* 19, 730–781.
- Fick, C., Toldo, E.E., Puhl, E., 2018. Shell concentration dynamics driven by wave motion in flume experiments: insights for coquina facies from lake-margin settings. *Sediment. Geol.* 374, 98–114.
- Folk, R.L., 1962. Spectral subdivision of limestone types. In: Ham, W.E. (Ed.), *Classification of Carbonate Rocks. A Symposium*. vol. 1. AAPG Memoir, pp. 62–84.
- Figueiredo, A.M.F., 1981. Depositional systems in the lower Cretaceous Morro do Chaves and Coqueiro Seco Formations, and their relationship to petroleum accumulations, middle rift sequence, Sergipe Alagoas Basin, Brazil. In: PhD Thesis. The University of Texas, Austin, pp. 275–p.
- Flügel, E., 2004. *Microfacies of Carbonate Rocks. Analysis, Interpretation and Application*. Springer-Verlag, Berlin, Heidelberg, New York, pp. 976.
- Freundt, A., Strauch, W., Kutterolf, S., Schmincke, H.U., 2007. Volcanogenic tsunamis in lakes: examples from Nicaragua and general implications. *Pure Appl. Geophys.* 164, 527–545.
- Goldberg, K., Kuchle, J., Scherer, C., Alvarenga, R., Ene, P.L., Armelenti, G., De Ros, L.F., 2017. Re-sedimented deposits in the rift section of the Campos Basin. *Mar. Pet. Geol.* 80, 412–431.
- Gomes, P.O., Parry, J., Martins, W., 2002. The External High of the Santos Basin, southern

- Sao Paulo Plateau, Brazil: tectonic setting, relation to volcanic events and some comments on hydrocarbon potential. In: AAPG Search and Discovery Article 90022, AAPG Hedberg Conference, Stavanger, Norway, pp. 1–5.
- Harris, N.B., 2000. Toca carbonate, Congo basin: response to an evolving rift lake. In: Mello, M.R., Katz, B.J. (Eds.), *Petroleum Systems of South Atlantic Margin*. AAPG Memoir 73. AAPG, Tulsa, Oklahoma, USA, pp. 341–361.
- Herlinger, R., Zambonato, E.E., De Ros, L.F., 2017. Influence of diagenesis on the quality of Lower Cretaceous Pre-Salt lacustrine carbonate reservoirs from northern Campos Basin, offshore Brazil. *J. Sediment. Res.* 87 (12), 1285–1313.
- Jahnert, R., De Paula, O., Collins, L., Strobach, E., Pevsner, R., 2012. Evolution of a coquina barrier in Shark Bay, Australia by GPR imaging: architecture of a Holocene reservoir analog. *Sediment. Geol.* 281, 59–74.
- Kidwell, S.M., 1986. Models for fossil concentrations: paleobiological implications. *Paleobiology* 12, 6–24.
- Kidwell, S.M., Bosence, D.W.J., 1991. Taphonomy and time-averaging of marine shelly faunas. In: Allison, P.A., Briggs, D.E.G. (Eds.), *Taphonomy. Releasing the Data Locked in the Fossil Record*. Plenum Press, New York, pp. 115–209.
- Kidwell, S.M., Fursich, F.T., Aigner, T., 1986. Conceptual framework for the analysis and classification of fossil concentrations. *Palaios* 1, 228–238.
- Kinoshita, E.M., 2007. Modelagem sísmica-geométrica de fácies dos carbonatos lacustres do Mb. Morro do Chaves, Bacia de Sergipe-Alagoas 97 MS Dissertation, Instituto de Geologia, Universidade Federal do Paraná, Curitiba.
- Massari, F., D'Alessandro, A., Davaud, E., 2009. A coquinoïd tsunamiite from the Pliocene of Salento (SE Italy). *Sediment. Geol.* 221 (1–4), 7–18.
- Mello, M.R., 2008. The Super Giant Great Lagoa Feia Petroleum System: the New Frontier of Exploration in the Pre-salt Sequences of the Great Campos Basin, Brazilian. AAPG Search and Discovery Article. AAPG Annual Convention, San Antonio, Texas.
- Mizuno, T.A., Mizusaki, A.M.P., Lykawka, R., 2018. Facies and paleoenvironments of the Coqueiros Formation (Lower Cretaceous, Campos Basin): a high frequency stratigraphic model to support pre-salt “coquinas” reservoir development in the Brazilian continental margin. *J. South Am. Earth Sci.* 88, 107–117.
- Morton, R.A., Gelfenbaum, G., Jaffe, B.E., 2007. Physical criteria for distinguishing sandy tsunami and storm deposits using modern examples. *Sediment. Geol.* 200, 184–207.
- Mulder, T., Alexander, J., 2001. The physical character of subaqueous sedimentary density flows and their deposits. *Sedimentology* 48, 269–299.
- Muniz, M.C., 2013. Tectono-Stratigraphic Evolution of the Barremian-Aptian Continental Rift Carbonates in Southern Campos Basin, Brazil. PhD Thesis. Royal Holloway University of London, Londres, pp. 324.
- Nagle, J.S., 1967. Wave and current orientation of shells. *J. Sediment. Petrol.* 37 (4), 1124–1138.
- Nutz, A., Schuster, M., Ghienne, J.-F., Roquin, C., Bouchette, F., 2018. Wind-driven waterbodies: a new category of lake within an alternative sedimentologically-based lake classification. *J. Paleolimnol.* 59, 189–199.
- Petersohn, E., Abelha, M., 2013. *Libra, Brazil pre-salt, geological assessment. National agency of petroleum natural gas and biofuels (ANP)*. Available in: http://www.brasil-rounds.gov.br/arquivos/Seminarios_P1/Apresentacoes/partilha1_tecnico_ambiental_ingles.pdf, Accessed date: March 2015.
- Pozo, M., Casas, J., 1999. Origin of kerolite and associated Mg clays in palustrine-lacustrine environments. The Esquivias deposit (Neogene Madrid Basin, Spain). *Clay Miner.* 34, 395–418.
- Rangel, H.D., Martins, C.C., 1998. Main exploratory compartments, Campos basin. In: *Searching For Oil and Gas in the Land of Giants*. Search, Rio de Janeiro, Schlumberger, pp. 32–40.
- Rehim, H.A.A.A., Pimentel, A.M., Carvalho, M.D., Monteiro, M., 1986. Talco e estevensita na Formação Lagoa Feia da Bacia de Campos – possíveis implicações no ambiente deposicional. *Brazilian Congress of Geology* 34, 416–425 Goiania, Annals 1.
- Schaffer, W., 1972. *Ecology and Paleogeology of Marine Environments*. The University of Chicago Press, Chicago, pp. 568pp.
- Schuster, M., Nutz, A., 2018. Lacustrine wave-dominated clastic shorelines: recent to ancient landforms and deposits from the lake Turkana basin (East African rift system, Kenya). *J. Paleolimnol.* 59, 221–243.
- Selley, R.C., 1970. *Ancient Sedimentary Environments*. Chapman and Hall, London, pp. 237.
- Segev, A., 2002. Flood basalts, continental breakup & the dispersal of Gondwana: evidence for periodic migration of upwelling mantle flows (plumes). *European Geosciences Union, Stephan Mueller, Special Publication* 2, 171–191.
- Soreghan, M.J., Cohen, A.S., 1996. Textural and compositional variability across littoral segments of Lake Tanganyika: the effect of asymmetric basin structure on sedimentation in large rift lakes. *Am. Assoc. Pet. Geol. Bull.* 80, 382–409.
- Tavares, A.C., Borghi, L., Corbett, P., Nobre-Lopes, J., Camara, R., 2015. Facies and depositional environments for the coquinas of the Morro do Chaves Formation, Sergipe-Alagoas Basin, defined by taphonomic and compositional criteria. *Braz. J. Genet.* 45 (3), 415–429.
- Tiercelin, J.J., Cohen, A.S., Soreghan, M.J., Lezzar, K.E., 1994. Pleistocene-Modern Deposits of the Lake Tanganyika Rift Basin, East Africa: a Modern Analog for Lacustrine Source Rocks and Reservoirs. SEPM Special Publications, AAPG, Denver Meeting, pp. 37–59.
- Tigre, C.A., Schaller, H., Del Lucchese Jr., , Possato, S., 1993. Pampo, Linguado, and Bajejo fields: their discoveries. In: *Appraisals, and Early Production Systems*. OTC 4627, Offshore Technology Conference, Houston, Texas, pp. 407–411.
- Tosca, N., Wright, V.P., 2015. Diagenetic pathways linked to labile Mg-clays in lacustrine carbonate reservoirs: a model for the origin of secondary porosity in the Cretaceous Pre-salt Barra Velha Formation, offshore Brazil. *The Geological Society of London Special Publication* 435, 33–46.
- Winter, W.R., Jahnert, R.J., França, A.B., 2007. Bacia de Campos. *Bol. Geociencias Petrobras* 15, 511–529.
- Zalan, P.V., do Carmo, M., Severino, G., Rigoti, C.A., Magnavita, L.P., Bach de Oliveira, J.A., Vianna, A.R., 2011. An Entirely New 3D-View of the Crustal and Mantle Structure of a South Atlantic Passive Margin – Santos, Campos and Espírito Santo Basins, Brazil. *American Association of Petroleum Geologists Annual Convention and Exhibition, Houston, TX, USA 10–13 April 2011, Search and Discovery Article #30177*. http://www.searchanddiscovery.com/documents/2011/30177zalan/ndx_zalan.pdf.
- Zhang, X., Scholz, C.A., 2015. Turbidite systems of lacustrine rift basins: examples from the lake kivu and lake albert rifts, East Africa. *Sediment. Geol.* 325, 177–191.
- Zuffa, G.G., 1980. Hybrid arenites: their composition and classification. *J. Sediment. Petrol.* 50, 21–29.
- Azambuja N.C., Arienti L.M., Cruz F.E.G. 1998. Guidebook to the Rift-Drift Sergipe-Alagoas, Passive Margin Basin, Brazil. In: *The 1998 AAPG International Conference and Exhibition, Rio de Janeiro, AAPG*, 113p.
- Carvalho, M.D., Praça, U.M.; Dias, J.L.; Silva-Telles Jr., A.C., Horschutz, P., Hessel, M.H., Hanashiro, M., Scuta, M.S., Barbosa, A.S.C., Freitas, L.C.S., Sayd, A.D. 1995. Coquinas da Formação Lagoa Feia da Bacia de Campos: estudos sedimentológicos na caracterização da qualidade do reservatório. *PETROBRAS, CENPES - Depex. Internal Report*, 3 v.